Chapter 11

Ladle Refining and Vacuum Degassing

G. J. W. Kor, Scientist, The Timken Co. (Retired)
P. C. Glaws, Senior Research Specialist, The Timken Co.

The treatment of steel in the ladle started approximately 45 years ago when the first ladle-to-ladle and ladle-to-ingot mold vacuum degassing processes for hydrogen removal appeared on the scene. In the late 1950s more efficient vacuum degassers such as the Dortmund Hoerder (DH) and Ruhrstahl-Heraeus (RH) processes became popular. In the middle 1960s degassing processes such as vacuum arc degassing (VAD), the ASEA-SKF process, and the vacuum oxygen decarburization (VOD) process for treating high-chromium steels were successfully implemented. Converter processes such as the argon oxygen decarburization (AOD) process were introduced in the early 1970s. The AOD process is now the preferred route in many specialty steel and stainless steel shops.

Granulated flux injection into the liquid steel, combined with argon stirring, started in the early 1970s. This was soon followed by the application of cored-wire feeding of alloying elements for better control of composition and inclusion morphology. A good overview of the various developments was given by Nijhawan[1], while an extensive review of the thermodynamic and kinetic principles underlying the various secondary steelmaking processes was prepared by Lange.[32]

All the aforementioned innovations have had a pronounced effect on the steelmaking process, particularly with respect to the vessel or the furnace in which the steel is produced. For example, the implementation of ladle metallurgy and its related aspects enabled electric furnace steelmakers to use their furnaces as fast melters without the need to perform any refining in the furnace. In addition, ladle refining and degassing make it possible for the steelmaker to exert much tighter control over the properties of the final product through improved accuracy in the composition of the final product as well as its cleanliness and by being able to control inclusion morphology.

The contents of this chapter are arranged according to the sequence of operations in a steelmaking shop, i.e. starting with tapping the furnace, followed by reheating, refining, inclusion modification and degassing. Where appropriate, the underlying metallurgical principles of each operation will be discussed in terms of reaction equilibria and kinetics as well as fluid dynamics. In preparing this chapter frequent reference has been made to a recently published book by Turkdogan.[2]

11.1 Tapping the Steel

11.1.1 Reactions Occurring During Tapping

During tapping of the steel, air bubbles are entrained into the steel where the tap stream enters the bath in the tap ladle. The quantity of air entrained into the steel increases with the increasing free fall height of the tap stream as was demonstrated with the aid of water model studies.[2] The entrainment of a gas such as air into a falling stream of liquid steel has been the subject of a number of studies.[3–6] However, a reliable prediction of the quantity of air entrained into a stream of liquid steel during tapping is difficult because of the assumptions that have to be made.

The nitrogen contained in the air entrained by the steel will be absorbed by the liquid steel depending on the extent to which the reaction

$$N_2\ (g)\ \rightarrow\ 2\ [N] \tag{11.1.1}$$

will proceed to the right; the symbol within the square brackets refers to nitrogen dissolved in the steel. It is well-known that surface active solutes such as oxygen and sulfur impede the kinetics of nitrogen absorption by the steel. The higher the concentration of dissolved oxygen and/or sulfur, the lower is the extent of nitrogen absorption. This is illustrated in Fig. 11.1 where the effect of deoxidation practice on the nitrogen pickup during tapping of an electric furnace is shown.[7] For deoxidized steels the average nitrogen pickup during tap is significantly higher than for non-deoxidized steels. The same effect is shown in Fig. 11.2 where the nitrogen pickup during tapping of 220 tonne oxygen converter heats is depicted as a function of the dissolved oxygen content for steels containing approximately 0.01% sulfur.[2] The data in Fig. 11.1 and Fig. 11.2 are in complete accord.

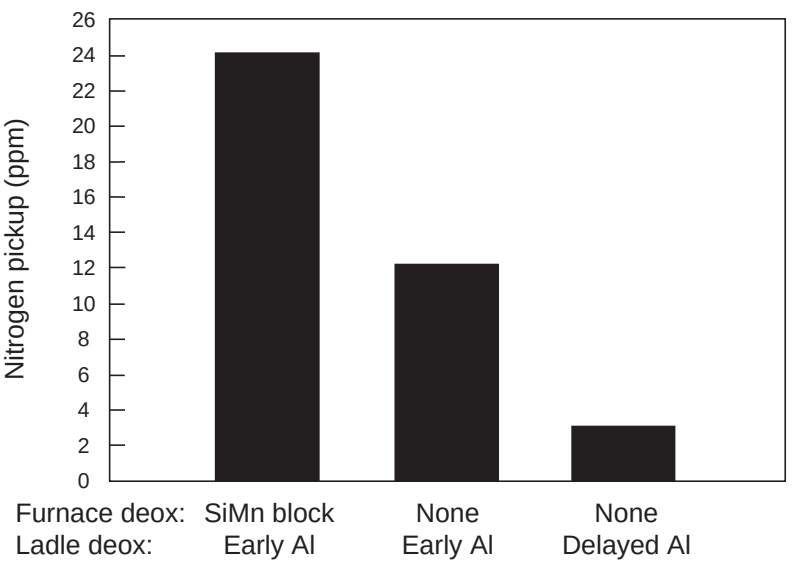

Fig. 11.1 Effect of deoxidation practice on nitrogen pickup during tap. *From Ref. 7*

Other sources contributing to the nitrogen pickup during or shortly after tap are: petroleum coke, when used for recarburization and various ferroalloys, particularly ferrotitanium, ferrovanadium and low and medium-carbon ferrochromium.

Ladle additions often contain moisture which reacts with the liquid steel according to the following reaction:

$$H_2O\ \rightarrow\ 2[H]\ +\ [O] \tag{11.1.2}$$

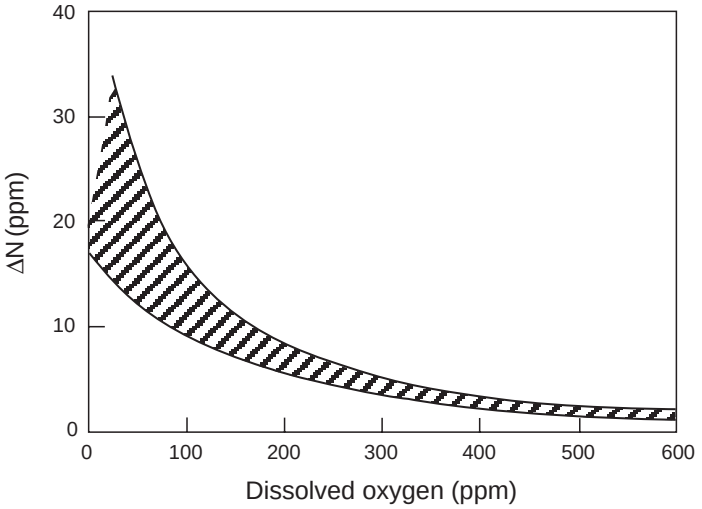

Fig. 11.2 Nitrogen pickup during tapping of 220 tonne heats as affected by the extent of deoxidation in the tap ladle. *From Ref. 2.*

It is seen from this equation that the extent of hydrogen pickup will be more pronounced for a fully deoxidized steel in which the dissolved oxygen content is low.

Of the various ferroalloys, ferromanganese is probably the major contributor of hydrogen.

11.1.2 Furnace Slag Carryover

It is generally unavoidable that a quantity of furnace slag is carried over into the tap ladle during tapping. The furnace slag generally contains a high concentration of FeO and MnO and therefore (in an untreated form) is not suitable for use as a refining slag. Accordingly, methods to minimize the amount of furnace slag carryover have been developed and implemented; Szekely et al. discuss various methods for BOFs and EAFs.[8] These include locating the taphole in the barrel of the converter sometimes in conjunction with the use of a ceramic sphere to block off the taphole towards the end of tap. In electric arc furnaces the first improvement was the use of submerged tapholes, later followed by the widespread implementation of eccentric bottom tapholes, which are now common in modern arc furnaces.

In older shops, inadequately equipped to control furnace slag carryover, slag raking is often practiced to remove the furnace slag. A good slag-free surface is attainable by careful raking. According to Hoeffken et al. raking is usually accompanied by a temperature loss of approximately 2.5°C (~5°F) per minute of treatment time and a metal loss of approximately 0.2%,[9] raking times are typically of the order of ten minutes. For best results it is recommended that the steel be tapped open, then raked and covered with the synthetic ladle slag and finally deoxidized.

As a result of furnace slag carryover into the tap ladle, oxidation of aluminum and silicon present in the ladle additions occurs through reactions with less stable oxides (e.g. iron oxide and manganese oxide) present in the furnace slag. Another consequence of furnace slag carryover is phosphorus reversion from the slag to the steel, particularly when the steel is fully deoxidized.

To be able to predict the aluminum and silicon losses as well as the anticipated degree of phosphorus reversion, it is necessary to know the quantity of furnace slag carried over into the tap ladle. Kracich et al. describe a sensor to measure the depth of the slag layer in a ladle.[10] These data provide accurate feedback to the melter and assist him in controlling the amount of furnace slag carryover.

11.1.2.1 Aluminum and Silicon Losses

The reactions of aluminum and silicon dissolved in the steel with the iron and manganese oxide in the slag and with the fallen converter skull may be represented by the following general reaction:

$$\text{Fe (Mn) } O_x + \text{Al (Si)} = \text{Fe (Mn)} + \text{Al (Si) } O_x \qquad (11.1.3)$$

Using average molecular masses and assuming 80% Fe_3O_4 for the composition of the skull, Turkdogan[11] derived the following approximate emperical relation for the percentages of aluminum and silicon lost to the ladle slag for a 200 tonne steel bath in the ladle:

$$[\%\text{Al} + \%\text{ Si}]_s \approx 1.1 \times 10^{-6}\ \Delta\ (\%\text{FeO} + \%\text{MnO})\ W_{fs} + 1.1 \times 10^{-4}\ W_{sk} \qquad (11.1.4)$$

where W_{fs} and W_{sk} are the weights (kg) of the carried over furnace slag and the fallen converter skull, respectively and Δ(FeO + %MnO) is the decrease in oxide contents of the furnace slag during tapping.

11.1.2.2 Phosphorus Reversion

Furnace slag carryover generally results in phosphorus reversion from the slag to the steel, particularly when the steel is fully deoxidized. The general relationship for the increase in steel phosphorus content, Δ[%P], as a result of reversion from the slag is:

$$\Delta\,[\%P] = (\%P)\,(W_{fs} \;/\; W_b) \qquad (11.1.5)$$

where (%P) is the phosphorus content of the furnace slag and W_{fs} and W_b are the weights of the carried-over furnace slag and the steel bath in the ladle, respectively.

For OBM (Q-BOP) heats and low-carbon heats made in EAFs with oxygen injection, typical values for (%P) and Δ[%P] are approximately 0.3 and 0.003, respectively.[11,12] Substitution of these values into equation 11.1.5 gives $W_{fs}/W_b \approx 0.01$. In other words, when proper measures are taken to prevent excessive furnace slag carryover, the average quantity of carried-over converter or furnace slag is approximately 1% of the steel tapped. This quantity of slag carried over during tapping corresponds to a slag thickness in a 200 tonne ladle of 5.5 ± 3 cm, in general agreement with plant observations.[11]

Hoeffken et al.[9] observed that phosphorus reversion is more likely to occur when both the basicity, $\%CaO/\%SiO_2$, of the carryover slag is approximately 2 or lower and its iron oxide content is approximately 17% or lower. For iron oxide contents of approximately 25% or higher the phosphorus reversion is noticeably less, provided the slag basicity exceeds 2–2.5.

For heats that are tapped open, to which only ferromanganese and a small amount of aluminum are added, the steel is not sufficiently deoxidized to cause phosphorus reversion. In fact, in some cases of tapping open heats to which 0.3–0.6% manganese is added, the phosphorus content of the steel decreases by approximately 0.001% due to mixing of the carried-over furnace slag with the steel during tapping.[11]

11.1.3 Chilling Effect of Ladle Additions

Ferroalloys and fluxes added to the steel in the tap ladle affect the temperature of the steel in the ladle, usually resulting in a decrease in temperature. The effect of various alloying additions, including coke, on the change in temperature of the steel for an average bath temperature of 1650°C (3002°F) is summarized in Table 11.1. These data were calculated from the heat capacities and heats of solution of the various solutes.

Table 11.1 Effect of Alloying Additions on the Change in Temperature of the Steel in the Tap Ladle for an Average Bath Temperature of 1650°C (3002°F).

Addition to give 1% of alloying element at 100% recovery	Change in steel temperature ΔT, °C (°F)
Coke	–65 (–117)
FeCr (50%), high-C	–41 (–74)
FeCr (70%), low-C	–28 (–50)
FeMn, high-C	–30 (–54)
FeSi (50%)	~0 (~0)
FeSi (75%)	+14 (+25)

It can be seen from Table 11.1 that ferrosilicon is the only ferroalloy that, upon addition, does not result in a decrease in steel bath temperature; in fact, the use of FeSi (75%) results in an increase

in temperature. This is a consequence of the fact that the dissolution of silicon into liquid iron is exothermic, i.e. heat is liberated. Although FeSi (75%) usually costs more per unit weight of contained silicon than FeSi (50%), the use of the former material can be justified under certain conditions, particularly when relatively large quantities must be added and when the shop has no or limited reheating facilities such as ladle furnaces.

For aluminum-killed steels, the exothermic heat of the deoxidation reaction must be taken into account when calculating the effect of an aluminum addition to the tap ladle on the change in steel temperature. For example, when a steel containing 600 ppm of dissolved oxygen is deoxidized with aluminum, the heat generated by the deoxidation reaction results in a change in steel temperature of +19°C (+34°F). In other words, when the steel in the tap ladle is deoxidized with aluminum, the decrease in steel temperature as a result of tapping will be less by 19°C (34°F).

Flux and slag conditioner additions decrease the temperature of the steel in the ladle. The effect of these additions on the change in steel temperature as determined from the heat capacity data is summarized in Table 11.2.

Table 11.2 Change in Steel Temperature in the Tap Ladle as a Result of Various Flux Additions at a Rate of 1 kg/tonne Steel (2.0 lbs/ton).

Flux added (1 kg/tonne)	Change in steel temperature ΔT, °C (°F)
SiO_2	–2.5 (–4.5)
CaO	–2.0 (–3.6)
MgO	–2.7 (–4.9)
CaO•MgO (dolomite)	–2.3 (–4.1)
CaO•Al_2O_3 (Ca-aluminate)	–2.4 (–4.3)
CaF_2	–3.2 (–5.8)

When tapping aluminum-killed steels to which typical ladle additions of 10 kg lime and pre-fused calcium aluminate per tonne of steel (20 lbs/ton) are made, the decrease in steel temperature during tapping to a pre-heated ladle is 55–75°C (99–135°F). The heat loss due to the flux addition is approximately balanced by the heat generated by the deoxidation reaction with aluminum. Thus, in this particular practice the heat losses are almost entirely from radiation and conduction into the ladle lining.

11.2 The Tap Ladle

11.2.1 Ladle Preheating

In most oxygen and many EAF steelmaking shops the ladle lining consists of high-alumina bricks (70–80%Al_2O_3) while the slag line consists of magnesia bricks, usually containing approximately 10% carbon and small amounts of metallic additions such as aluminum, magnesium or chromium to minimize the oxidation of carbon. For many EAF shops the lining is dolomite. The refractory materials used in tap ladles are discussed in detail in Chapter 4 and will not be discussed here further,

Table 11.3 Heat Storage Capacity per Unit Volume of Various Refractory Materials at 1200 and 1500°C Relative to Magnesia (=100%), after Tomazin et al.[14]

Material	1200°C (2192°F)	1500°C (2732°F)
70% alumina	83%	85%
50% alumina	79%	82%
fireclay	73%	74%

except to make reference to a series of articles by Engel et al.[13] which represents a comprehensive overview of refractory materials and configurations employed in secondary steelmaking.

The thermal properties of various refractories used in ladles are summarized in Table 11.3 and Fig. 11.3.

It is seen from Fig. 11.3 that magnesia has a significantly higher thermal conductivity than the other refractory materials. Magnesia also has a higher heat storage capacity than the other materials as shown in Table 11.3. The properties of dolomite are similar to those of magnesia.

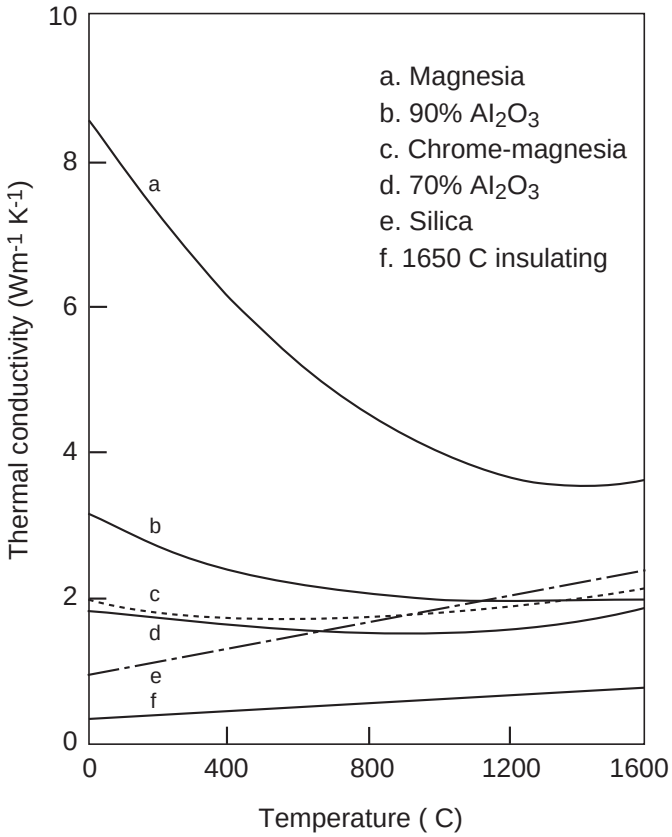

Fig.11.3 Thermal conductivity of refractory bricks used in ladle linings. *From Ref. 2.*

Because of the relatively high thermal conductivity of the refractories used in ladles, preheating of the ladle prior to its use is required to avoid excessive heat losses during tapping and during subsequent refining operations. Tomazin et al.[14] studied the effect of ladle refractories and practices on steel temperature control and developed a mathematical model to simulate a ladle which is used to supply liquid steel to a continuous caster. The model was used to evaluate the temperature increase of the hot and cold faces of a ladle during preheating. This is shown in Fig. 11.4 from which it is seen that the temperature of the hot face increases rapidly with time. However, the cold face temperature does not exceed 100°C (212°F) after preheating for approximately 5½ hours when the ladle is cold and dry initially.

The rate of rise of temperature of the hot face depends on the distance from the ladle top to the burner wall as well as on the thermal input from the preheater. A rapid heating rate should be avoided for the following reasons:

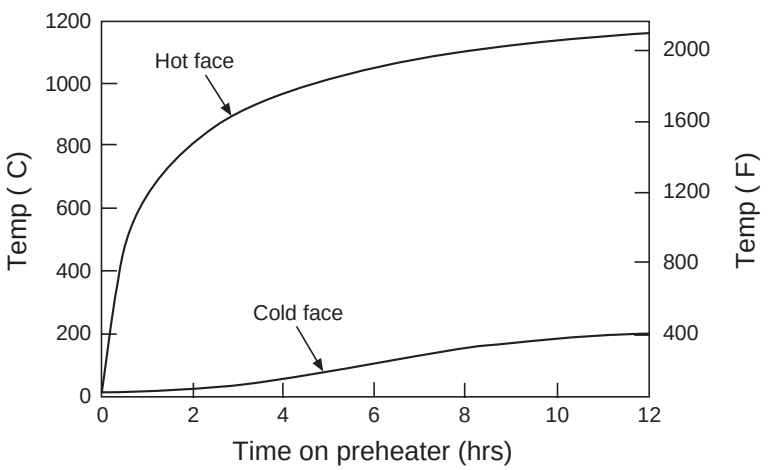

Fig. 11.4 Lining temperatures during preheating of a cold dry ladle. *From Ref. 14.*

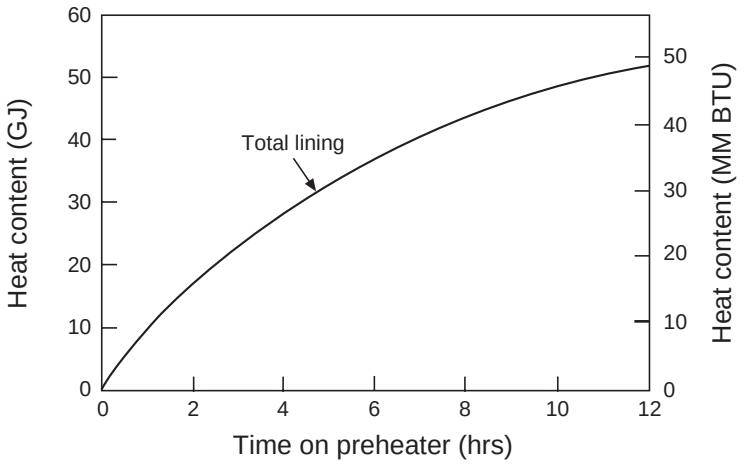

Fig. 11.5 Total heat content of a lining as a function of preheating time. *From Ref. 14.*

(i) Rapid heating results in a non-equilibrium temperature profile, i.e. a steep temperature gradient adjacent to the hot face.

(ii) Rapid heating causes extreme shell stresses.

(iii) The thermal shock resistance of the brick may not be high enough to withstand a rapid heating rate.

Another measure of the thermal condition of the ladle is the total heat content of the ladle brick. As shown in Fig. 11.5, the brick continues to absorb heat at a significant rate for up to twelve hours. At this time the ladle brick contains in excess of 90% of the maximum heat content that can be attained once steady state has been reached after 17–18 hours of preheating.

After preheating the ladle is moved to the converter or the furnace. This causes a decrease in the temperature of the hot face. The temperature decrease must be taken into account when adjusting the tap temperature. The required adjustment in tap temperature is shown as a function of the time elapsed between the end of preheating and the start of tapping for two hot face temperatures, Fig. 11.6.

11.2.2 Ladle Free Open Performance

Upon arrival of the ladle at the continuous caster tundish, it has to be opened to allow the steel to flow into the tundish. When the ladle slide gate is stroked open and steel starts to flow without operator assistance, the procedure is classified as 'free open'. If poking or oxygen lancing is nec-

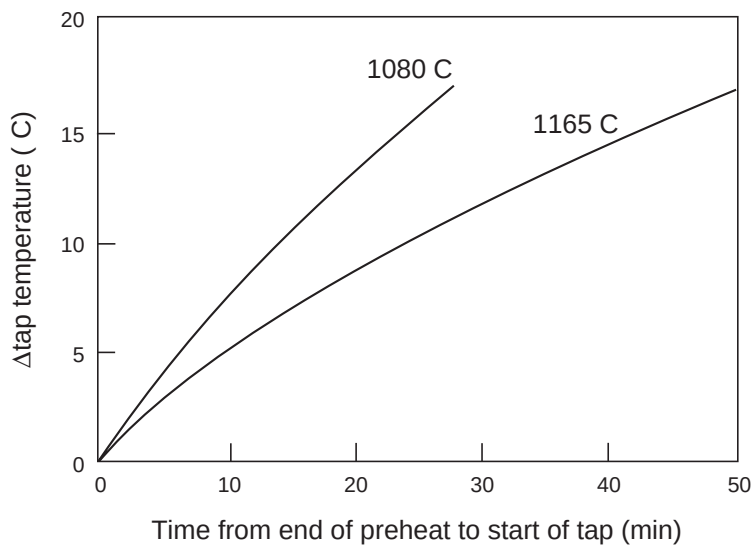

Fig. 11.6 The effect of cooling time for two different preheat temperatures on the tap temperature adjustment; ladle not covered between end of preheat and tap. *From Ref. 14.*

essary to open the ladle, the process is classified as 'assisted open'. When all attempts to open the ladle are unsuccessful, it is classified as 'non-free open'. These classifications were taken from Vitlip[15] who undertook a comprehensive study of ladle free open performance.

According to Vitlip[15] there are several factors that determine the opening performance of a ladle. The most dominant factor is the residence time of the steel in the ladle followed by the ladle preheat practice, the elapsed time between the end of stirring and the opening of the ladle at the caster, the cycle time for an empty ladle and the argon stirring practice. The relative effect of these factors on the percentage of free open ladles is summarized in Table 11.4.

Table 11.4 Percentage of Free Open Ladles as Affected by Various Factors, after Vitlip.[15]

Factor	Free Open	
Steel residence time in the ladle	< 5 hr, 85%	> 5 hr, 80.8%
Ladle preheat practice	normal cycle, 98.2%	repair, 90.9%
Time between end of stirring	< 20 min, 98.4%	> 20 min, 94.1%
Empty ladle cycle time	< 2 hr, 98.7%	> 2 hr, 97.0%
Argon stirring practice	bottom, 98.5%	top, 97.9%

11.2.2.1 Steel Residence Time in the Ladle

The residence time in the ladle is defined as the elapsed time between tapping and the opening of the ladle at the tundish. Under the operating conditions prevailing at the Wheeling-Pittsburgh Steel Corporation this time is 80 min.[15] However, longer residence times are not uncommon whenever problems are encountered at the caster. It can be seen from Table 11.4 that a residence time in the ladle longer than five hours results in a significant decrease in free open performance. Long residence times in the ladle cause partial sintering of the nozzle fill material due to extended exposure to liquid steel temperatures.

11.2.2.2 Ladle Preheat Practice

The ladle preheat practices at Wheeling-Pittsburgh were examined for ladles returned to service following repair.[15] The data in Table 11.4 show that the free open performance is worse for repaired ladles compared with those that follow the normal cycle, indicating an inadequate preheat practice for repaired ladles.

11.2.2.3 Elapsed Time Between End of Stirring and Opening

The data in Table 11.4 show that the time elapsed between the end of stirring at the trim station and the opening of the ladle at the tundish is important. The longer the time without stirring the worse is the free opening performance.

11.2.2.4 Empty Ladle Cycle Time

The empty ladle cycle time is the elapsed time between closing the ladle at the caster at the end of a cast and the time the ladle is filled again at tap. The practice at Wheeling-Pittsburgh was not to preheat the ladles when they were being rotated between the caster and the converter. However, the rate of rotation could vary significantly because of delays. The data in Table 11.4 show that an empty ladle cycle time longer than two hours leads to a decrease in free open performance.

11.2.2.5 Argon Stirring Practice

Today most ladles are equipped with bottom plugs for argon bubbling. Whenever the plug is out of commission, it may be necessary to provide the required stirring via a top lance. The data in Table 11.4 show that top stirring with argon results in a slightly decreased free open performance.

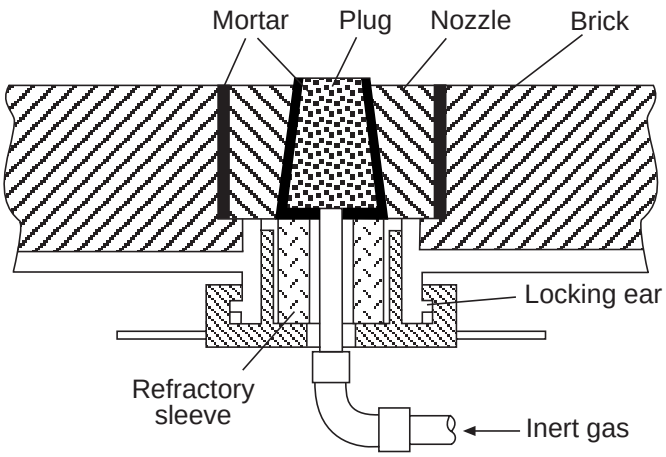

Fig. 11.7 Porous plug assembly in the bottom of a ladle. *From Ref. 2.*

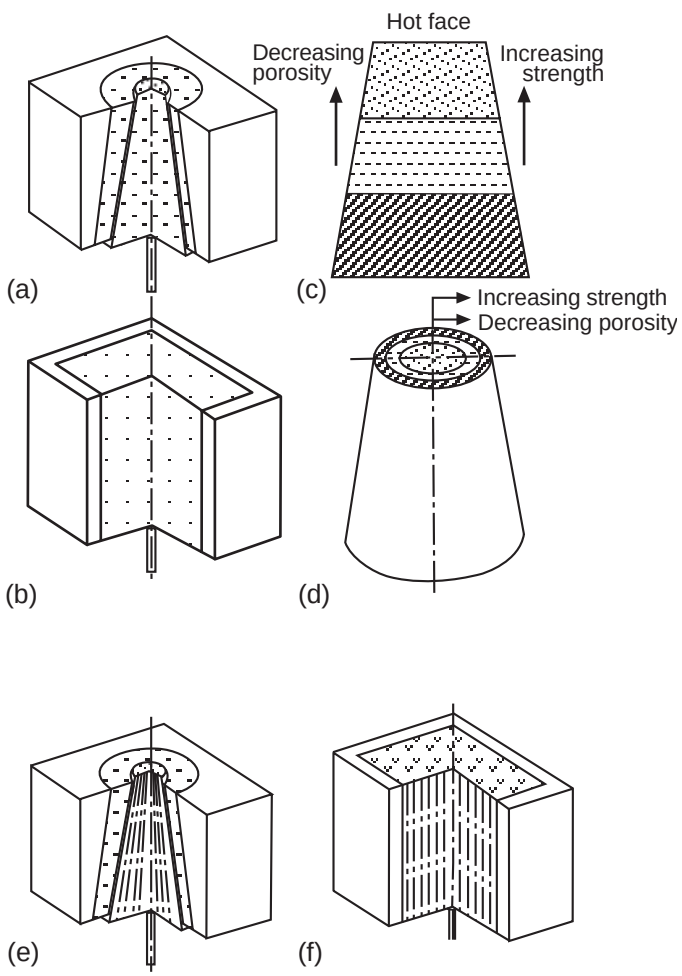

Fig. 11.8 Standard shapes of isotropic plugs: (a) and (b). Component plugs: sliced (e), concentric (d). Capillary plugs: conical (e) rectangular (f). *From Refs. 16 and 17*

Vitlip[15] studied the effect of a number of other factors on free open performance, the details of which may be found in the cited reference.

11.2.3 Stirring in Ladles

To achieve a homogeneous bath temperature and composition, the steel in the ladle is most often stirred by means of argon gas bubbling. For moderate gas bubbling rates, e.g. less than 0.6 Nm^3/min (~20scfm) porous refractory plugs are used, usually mounted in the bottom of the ladle. A schematic illustration of a porous plug assembly in the ladle bottom is shown in Fig. 11.7.

Anagbo and Brimacombe[16] discussed some typical examples of various plugs, shown in Fig. 11.8. As can be seen, porous plugs have either a conical or a rectangular shape. The conically shaped plug is easier to change should the plug wear out before the lining. Rectangular plugs are geometrically compatible with the surrounding bricks and can be used to advantage in cases where the plug life is comparable with that of the lining. The performance and life of isotropic plugs can be improved by producing the element in two or three components stacked together with metal inserts.[17] The primary advantage of the so-called directional-porosity or capillary plug, shown in Fig. 11.8(e) and (f), is that the plug can be made of the same dense refractory as the lining brick, or even denser. This results in increased hot compression strength, greater resistance to erosion and a longer service life. Disadvantages of capillary plugs are that they are more prone to infiltration by liquid steel upon loss of argon gas pressure. More details regarding the configurations of plugs and the modeling of porous plug operations can be found in the cited references.[16,17]

Some melt shops utilize electromagnetic induction stirring in the ladles.

Some reported features of induction stirring in the ladle include better stirring homogeneity (especially near the ladle bottom), the ability to reverse the direction of the stirring forces (useful for alloy additions) and stirring without breaking slag cover and exposing steel to the ambient oxidizing atmosphere. These benefits are offset by the high capital cost, including ladles equipped with stainless steel panels comprising at least 1/3 of the ladle shell and the need for auxiliary gas stirring for adequate hydrogen removal.

11.2.3.1 Stirring Power and Mixing Times

Homogenization of bath temperature and composition by gas bubbling is primarily caused by the dissipation of the buoyant energy of the injected gas. The thermodynamic relationship describing the effective stirring power of a gas was derived by Pluschkell.[18] The following equation for the stirring power is derived from Pluschkell's relationship:

$$\dot{\varepsilon} = 14.23 \left(\frac{\dot{V} T}{M} \right) \log \left(\frac{1 + H}{1.48\ P_o} \right) \qquad (11.2.1)$$

where:

$\dot{\varepsilon}$	=	stirring power, W/tonne
$\dot{V}$	=	gas flowrate, Nm^3/min
T	=	bath temperature, K
M	=	bath weight, tonne
H	=	depth of gas injection, m
P_o	=	gas pressure at the bath surface, atm

The stirring time to achieve 95% homogenization is defined as the mixing time τ. There have been numerous experimental and theoretical studies dealing with mixing phenomena in gas-stirred systems. Mazumdar and Guthrie[19] published a comprehensive review on the subject. The following relationship expressing the mixing time, τ, in terms of the stirring power, $\dot{\varepsilon}$ (W/tonne), ladle diameter, D(m), and depth of injection, H(m), was obtained from the work of Mazumdar and Guthrie.[20]

$$\tau(s) = 116\ (\dot{\varepsilon})^{-1/3}\ (D^{5/3}\ H^{-1}) \qquad (11.2.2)$$

Mixing times calculated from equations 11.2.1 and 11.2.2 are shown in Fig. 11.9 for the simplified case of D = H. The mixing times shown in Fig. 11.9 are in good agreement with those calculated from other correlations.[21,22] It can be seen from Fig. 11.9 that a 200 tonne heat will be homogenized in 2–2½ minutes after bubbling with argon at a flow rate of 0.2 Nm^3/min (~7 scfm).

The effect of the location of the bottom stirring plug on mixing times was studied by several authors.[23,24] The general finding was that the mixing time is decreased by placing the bottom plug off-center, e.g. at mid-radius.

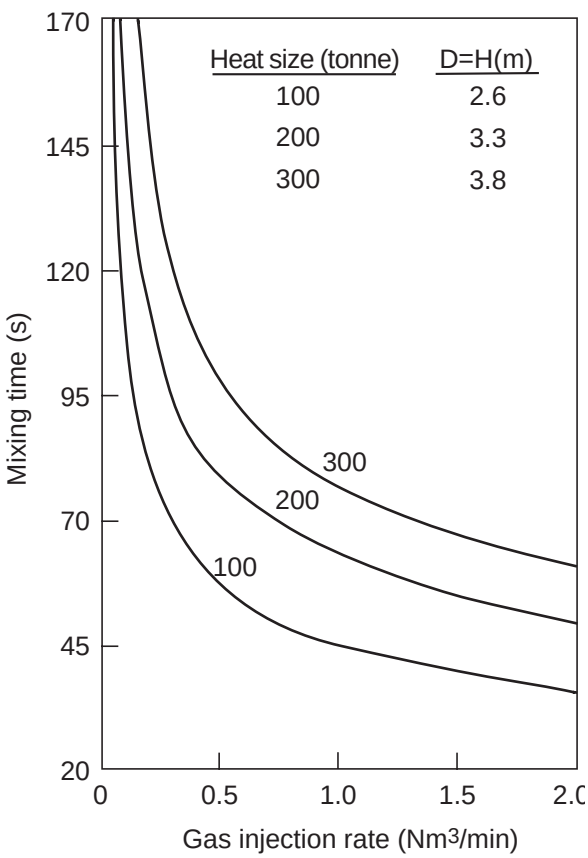

Fig. 11.9 Calculated mixing times for 100, 200 and 300 tonne heat sizes.

According to Mietz and Oeters[23] a stirring plug placed in the center of the ladle bottom generates a toroidal loop of metal flow in the upper part of the bath while a dead zone is created in the lower part, resulting in longer mixing times. Eccentrically located bottom plugs give rise to extensive circulation of metal throughout the entire bath, avoiding dead zones and leading to shorter mixing times.

11.2.3.2 Slag–Metal Reaction Rates in Gas-Stirred Melts

Numerous experimental studies to investigate slag–metal gas reactions in gas-stirred ladle systems under a variety of experimental conditions have been performed. Reviews on this subject were prepared by Mazumdar and Guthrie[19], Emi[25] and Asai et al.[26] For most slag–metal reactions the rates are controlled primarily by mass transfer of the reactants and products across the slag-metal interface. In stirred systems such as a steel bath in a ladle stirred by argon, the slag–metal interfacial area is affected by the degree of agitation in the bath which, in turn, is determined by the stirring power.

11.2.3.2.1 Desulfurization During desulfurization of the steel in the ladle, the mixing of slag and metal is achieved by argon bubbling and the rate of desulfurization is described by equation 2.10.19 in Chapter 2.

The overall rate constant is related to the average mass transfer coefficient, m_S, the slag–metal interfacial area, A, and the steel both volume, V, by the following expression:

$$k_S = m_S \left(\frac{A}{V} \right) \tag{11.2.3}$$

It has been shown that:

$$k_s \propto \varepsilon^n \tag{11.2.4}$$

where the exponent n may vary between 0.25 and 0.30, depending on the specific system under consideration.[26]

From pilot plant tests with 2.5 tonne heats[26] to study desulfurization, it was found that at moderate gas bubbling rates, corresponding to $\dot{\varepsilon} < 60$ W/tonne, there was little or no slag–metal mixing, hence the rate of desulfurization was slow. For higher stirring rates corresponding to $\dot{\varepsilon} > 60$ W/tonne, better mixing of slag and metal was achieved and the rate constant for desulfurization increased accordingly. The results of these experiments are summarized in Fig. 11.10 from which the following approximate relationships between the overall rate constant and the stirring power are derived:

$$\begin{aligned} k_S\ (\text{min}^{-1}) &\approx 0.013\ (\varepsilon)^{0.25} \text{ for } \varepsilon < 60 \text{ W/tonne} \\ k_S\ (\text{min}^{-1}) &\approx 8.10^{-6}\ (\varepsilon)^{2.1} \text{ for } \varepsilon > 60 \text{ W/tonne} \end{aligned} \tag{11.2.5}$$

It should be stressed that these are empirical correlations. The value of k_s depends on the energy dissipation per unit area at the slag–metal interface, the properties of the slag and the amount of the slag.

The abrupt change in overall rate constant for values of the stirring power at approximately 60 W/tonne is explained[8] by the fact that an increase in the energy input rate results in increased emulsification of slag and metal, leading to an increase in interfacial area, A, which, in turn, increases k_S.

11.2.3.2.2 Dephosphorization The removal of phosphorus from the steel by the ladle slag is governed by the same rate equation as that for sulfur removal, equation 2.10.19. Thus, the overall rate constant for dephosphorization is expected to have the same form as equation 11.2.4. That this is, in fact, the case was shown by Kikuchi et al.[27] who studied dephosphorization in the ladle with

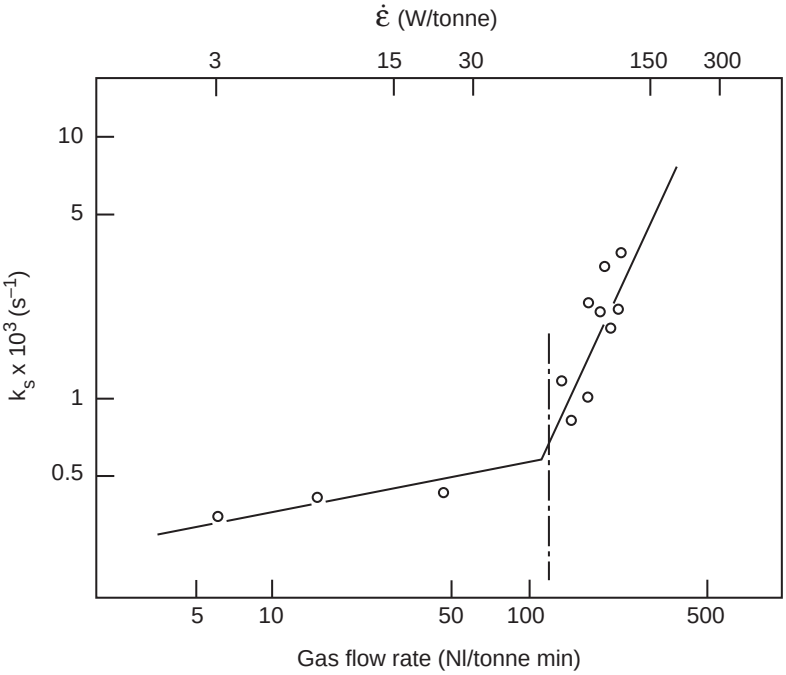

Fig. 11.10 Effect of gas flowrate and stirring power on the desulfurization rate constant. *From Ref. 26.*

$CaO–CaF_2–FeO$ slags in a 50 tonne VAD/VOD as well as in a 250 tonne ladle furnace facility. The overall rate constant can be represented by the following approximate relationship:

$$k_P\ (min^{-1}) \approx 0.019\ (\dot{\varepsilon})^{0.28} \qquad (11.2.6)$$

This expression is similar to that for k_S, valid for $\dot{\varepsilon} < 60$ W/tonne, equation 11.2.5. It is not clear why no abrupt change in k_P was observed for $\dot{\varepsilon} > 60$ W/tonne, as in the case of desulfurization, Fig. 11.10.

It is interesting to note that Kim and Fruehan[28] as well as Mietz et al.[29] observed that mass transfer between metal and slag is impeded when the stirring plug in the ladle bottom is located off-center. A stirring plug located in the center results in increased slag–metal emulsification with increasing gas flowrate. Eccentrically located stirring plugs create a slag-free zone, the so-called eye, close to the ladle wall. This affects the detachment of slag particles from the main slag phase and results in decreased emulsification.[29] The ultimate choice of location of the stirring plug in the bottom of the ladle would, therefore, appear to be determined by which aspect of stirring is more important for a given operation: good mixing characteristics, or the ability to achieve rapid desulfurization and/or dephosphorization. In most cases a compromise will have to be struck.

11.2.4 Effect of Stirring on Inclusion Removal

One of the objectives of stirring the steel in the ladle is the removal of non-metallic inclusions. Nakanishi and Szekely[30] studied the deoxidation kinetics of aluminum-deoxidized steels in 20 kg melts as well as in a 50 tonne ASEA-SKF furnace. The authors developed a model for inclusion removal based on the postulate that the decrease in total oxygen content is determined by the coalescence of oxide particles as the rate controlling step. The model is in essence a combination of a coalescence theory and an algorithm for turbulent recirculatory flows.

Engh and Lindskog[31] also presented a fluid mechanical model for inclusion removal from liquid steel. According to their model the total oxygen content after stirring time, t, is given by

$$\frac{C_t - C_f}{C_i - C_f} = e^{-at} \tag{11.2.7}$$

where

C_t = total oxygen content after the stirring time, t,

C_f = final total oxygen content after long stirring times (steady state),

C_i = initial total oxygen content,

α = the time constant for inclusion removal.

It must be stressed that equation 11.2.7 is an extremely simplified expression. The rate of inclusion removal depends on many factors including the inclusion type, refractory type, exact stirring conditions, etc.

From experiments with an inductively stirred 140 tonne melt[31] employing a range of values for the specific stirring power, $\dot{\varepsilon}$, the following approximate relationship can be obtained:

$$\alpha\,(\text{min}^{-1}) \approx \frac{\dot{\varepsilon}}{27} \tag{11.2.8}$$

The above expression is an approximation and is valid only for moderate induction stirring. If it is assumed that the final steady state total oxygen content, C_f, is small compared to C_i and C_t, combination of equations 11.2.7 and 11.2.8 gives:

$$\frac{C_t}{C_i} \approx e^{-\dot{\varepsilon}\tau/27} \tag{11.2.9}$$

11.3 Reheating of the Bath

The ever increasing pressure on steelmakers to lower operating costs and increase efficiency has made it necessary to make effective use of furnaces, BOF or EAF, and implement sequential continuous casting. These factors have prompted the installation of facilities for steel reheating, needed for the additional time required for steel refining and the adjustment of the temperature of the steel for uninterrupted sequential casting. The two methods for reheating steel in the ladle, arc reheating and injecting oxygen and aluminum or silicon, will be discussed separately.

11.3.1 Arc Reheating

Over time, several types of furnaces for arc reheating have been developed and commercialized. Examples are: ASEA-SKF, Daido-NKK, Finkl-Mohr, Fuchs, Lectromelt, MAN-GHH, Stein Heurty-S.A.F.E., etc. Some of these designs also have the capability for degassing of the steel. An important issue in arc reheating of a steel bath is whether the thermal energy which is supplied at, or near, the surface of the melt can be dispersed rapidly enough such that no significant temperature gradients are created within the steel in the ladle. Szekely[8] estimated that, in the absence of agitation, the Biot number is of the order of 300, indicative of significant temperature gradients in the steel bath. (The Biot number is defined as $N_{Bi} = hL/k_{eff}$, where h is the heat transfer coefficient between the arc and the bath, k_{eff} is the thermal conductivity of the steel and L is the bath depth.) In systems agitated either by induction stirring or gas bubbling, the Biot number is estimated to be of the order of 5.0, indicative of small temperature gradients even in agitated systems. Once the heat supply is discontinued, the temperature in gently agitated baths is expected to become uniform quite rapidly.[8]

Ruddlestone et al.[33] have compared the operating costs of an ASEA-SKF ladle furnace and a Fuchs ladle furnace and found that in both cases the primary cost factor is electric power, followed by electrode and refractory costs. This agrees with observations at The Timken Company.[34] These three cost categories will be discussed in more detail.

11.3.1.1 Electric Power

The heating efficiency, η, of arc heating is defined as:

$$\eta = \frac{\Delta T_{act}}{\Delta T_{th}} = 0.22\left(\frac{\Delta T_{act}}{E}\right) \tag{11.3.1}$$

where

ΔT_{act} = the actual temperature increase of the bath, °C,

ΔT_{th} = the theoretical temperature increase of the bath for 100% thermal efficiency, °C,

E = the energy consumption, kWh/tonne.

The heat capacity of liquid steel is 0.22 kWh/tonne°C; i.e. for 1 tonne of liquid steel $\Delta T_{th} = E/0.22$.

The heating efficiency increases with increasing bath weight, as shown in Fig. 11.11 obtained from data reported by Cotchen.[35] These data represent overall averages comprising a range of heating times. To minimize refractory consumption, heating times in ladle furnaces are kept as short as possible, typically around 15 min.[35] Further measures to shorten the reheating time and, thus, minimize refractory erosion are:[2] the use of a large capacity transformer, e.g. 35–40 MW for a 200 to 250 tonne heat, submerged arcing in the slag layer, argon stirring through a bottom porous plug at a flowrate of approximately 0.5 Nm^3/min (~18 scfm), a slag layer thickness of approximately 1.3 times the length of the arc (values of the arc length as a function of the secondary current are given by Turkdogan[2]).

11.3.1.2 Electrode Consumption

In general, electrode consumption in ladle furnaces increases with increasing cross sectional current density and heating time. The trends are shown in Fig. 11.12 which is based on data from a worldwide survey cited by Cotchen.[35] For the Stein Heurtey-S.A.F.E. facility in operation at the Faircrest steel plant of The Timken Company[34] the average electrode consumption is 0.2 kg/tonne for typical total reheat times of 20 minutes and average current densities of approximately 35 A/cm^2.

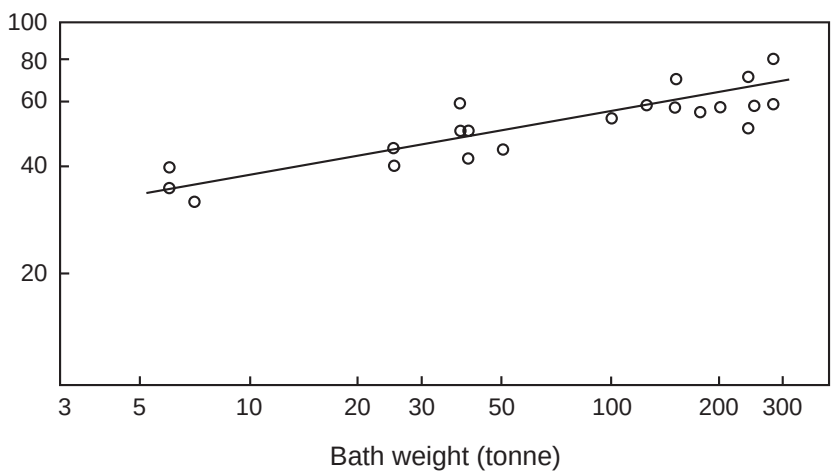

Fig. 11.11 Heating efficiency for various bath weights. *From Ref. 35.*

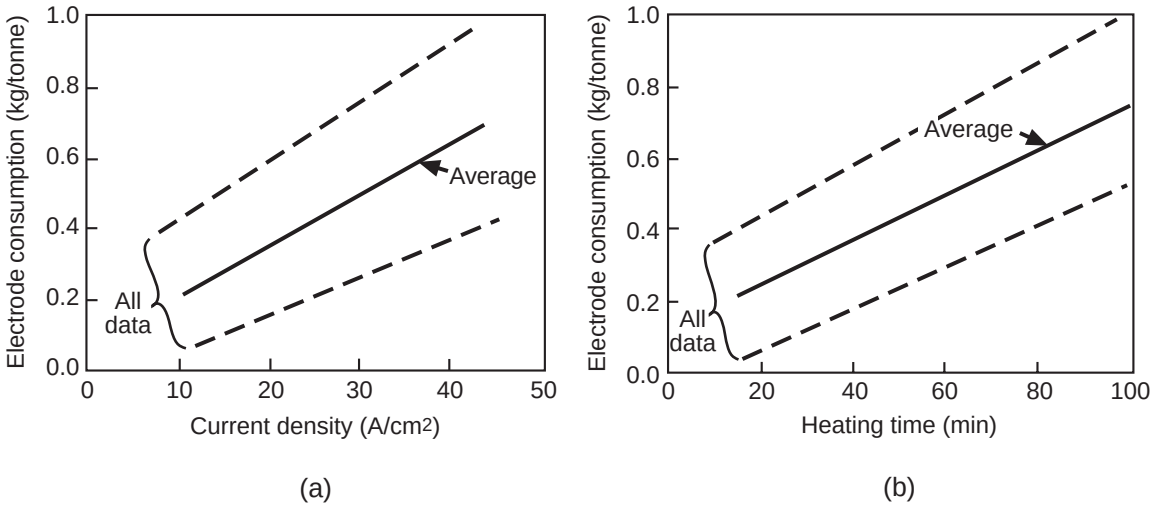

Fig. 11.12 Electrode consumption as affected by current density (a) and heating time (b). *From Ref. 35.*

11.3.1.3 Refractory Consumption

The refractory materials used in ladle furnace linings are similar for most steelmaking shops and applied in the same configurations, i.e. slagline, bottom and barrel. Thus, a comparison of refractory consumption data can be made for a variety of shops. The data in Fig. 11.13 show that the ladle life, expressed as the number of heats processed in a given ladle, increases with increasing bath weight.[35] At the Faircrest steel plant of The Timken Company, where 158 tonne (175 ton) heats are processed, the average ladle life is 45 heats.[34] It should be noted that the ladle refractory consumption in any given shop is strongly affected by the specific operating practice, as reflected by the considerable scatter in the data in Fig. 11.13. As mentioned before, submerged arc heating in the slag layer should result in lower refractory consumption.

11.3.2 Reheating by Oxygen Injection

Liquid steel can be reheated by oxidizing aluminum and/or silicon by means of oxygen injection through a lance. The heats generated for the reactions

$$2Al\ (R.T.) + \tfrac{3}{2}O_2\ (R.T.) \rightarrow Al_2O_3\ (1630°C) \qquad (11.3.2)$$

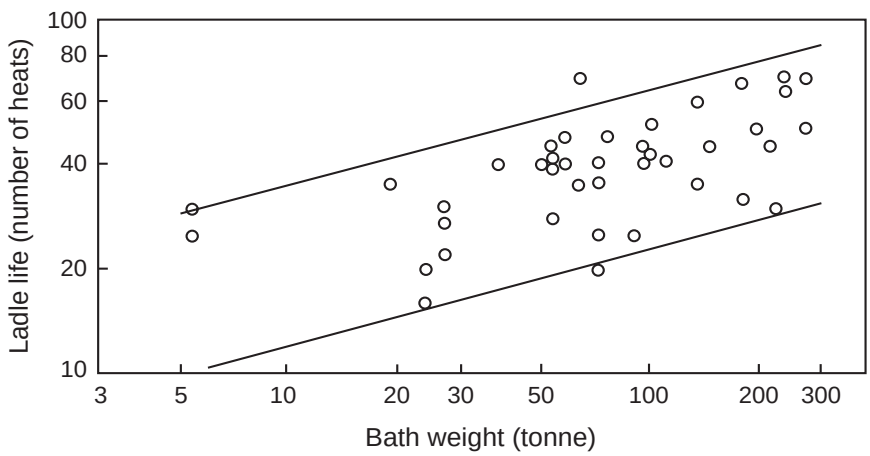

Fig. 11.13 Ladle life for various bath weights. *From Ref. 35.*

$$Si\ (R.T.) + O_2\ (R.T.) \rightarrow SiO_2\ (1630°C) \qquad (11.3.3)$$

are:[2] 27,000 kJ/kg Al for reaction 11.3.2 and 28,500 kJ/kg Si in Fe–75% Si for reaction 11.3.3.

The enthalpies are calculated from the thermodynamic data, taking into account that the reagents, aluminum and oxygen, must be heated from room temperature (R.T.) to the temperature of the bath (1630°C = 2966°F). On the basis of 100% thermal efficiency the bath temperature can be raised by 50°C (90°F) when 1 Nm^3O_2/tonne of steel is injected together with 1.46 kg Al/tonne or by injecting 1.2 Nm^3O_2/tonne together with 1.85 kg Fe–75% Si/tonne[2].

Reheating of steel in the ladle with submerged oxygen injection is being practiced at the steel plants of the Bethlehem Steel Corporation. Barbus et al.[36] have published data on reheating by submerged injection of oxygen into 270 tonne heats. From their data the temperature increase as a function of the specific quantity of oxygen (Nm^3/tonne of steel) injected can be obtained. This is shown in Fig. 11.14, line b. A comparison of the presented data with the maximum attainable temperature increase for 100% thermal efficiency (line a) indicates that reheating by means of submerged oxygen injection is approximately 70% efficient.

Miyashita and Kikuchi[37] presented data on the temperature increase in a 160 tonne RH-OB vessel. Their data are indicated by line c in Fig. 11.14 and indicate an average thermal efficiency of 20–30%. (Fruehan[68] quotes a reheating efficiency of approximately 80% for the RH-OB operation at the Oita works of the Nippon Steel Corporation.) Data for a 245 tonne RH-KTB vessel[38], in which the oxygen is supplied via a top lance instead of through submerged tuyeres as in the RH-OB, are indicated by line d in Fig. 11.14. The thermal efficiency for the RH-KTB process appears to be similar to that for submerged oxygen injection into the ladle.

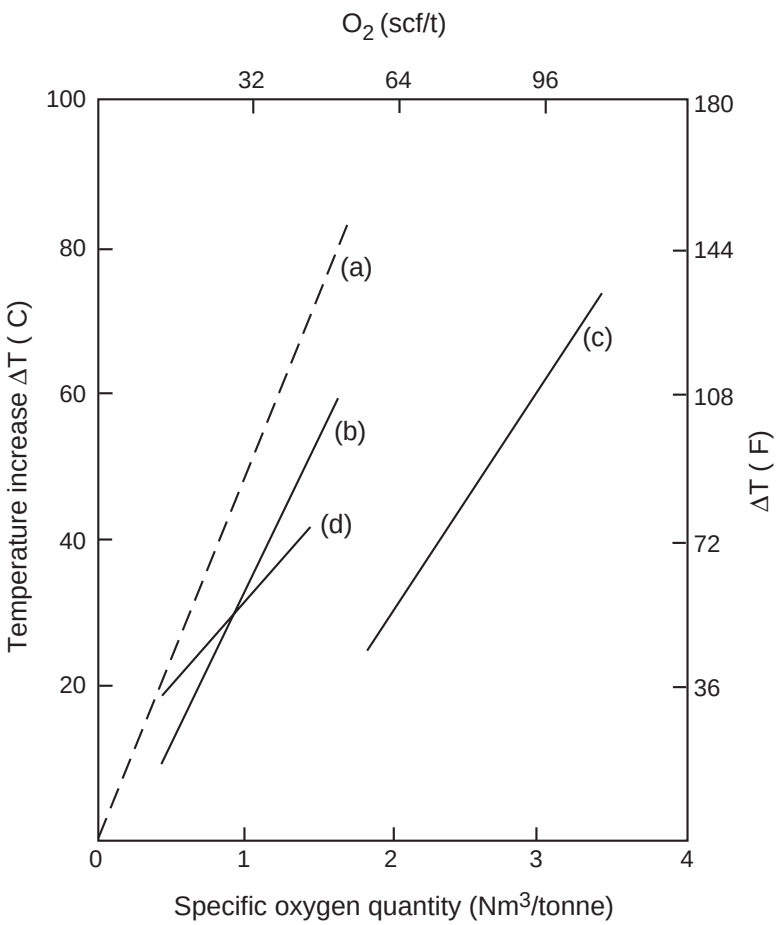

Fig. 11.14 Steel temperature increase by oxygen injection: (a) theoretical increase based on 100% thermal efficiency, (b) from data for submerged injection into 270 tonne heats (*From Ref. 36.*), (c) from data for 160 tonne RH-OB heats (*From Ref. 37.*), and (d) from data for 245 tonne RH-KTB heats (*From Ref. 38.*).

A comparison of total oxygen contents measured in slabs cast from oxygen-reheated heats and heats that were not reheated showed no significant differences between the two sets of values.[36] In addition, Griffing et al.[39] compared the inclusion ratings in rail-grade steels produced from oxygen-reheated steels and heats that were not reheated and found no significant differences between the two. These authors recommend the addition of a synthetic ladle slag after reheating, followed by a thorough argon rinse to float out the alumina inclusions so they may become dissolved in the slag.

Jung et al.[52] studied the effect of reheating with aluminum and oxygen in the RH-OB process on the cleanliness of the final product. An increase in the total oxygen content during and shortly after oxygen blowing was observed. However, the total oxygen content in the final product was found to be similar for steels treated with oxygen and aluminum compared with those treated without oxygen blowing in the RH, provided the total bath circulation time in the RH-OB was sufficiently long.

11.4 Refining in the Ladle

The refining of steel in the ladle is broadly defined here as comprising the following operations: deoxidation, desulfurization, dephosphorization, controlled additions of alloying elements and inclusion modification. Each of these operations will be discussed in detail in the following sections.

11.4.1 Deoxidation

The first step in the refining sequence in the ladle is usually the deoxidation of the steel with ferromanganese, ferrosilicon, silicomanganese and aluminum. There are three categories of steel deoxidation.

(a) Steel deoxidized with ferromanganese to yield 100–200 ppm dissolved oxygen; these are usually resulfurized steel grades.

(b) Semi-killed steels deoxidized with:

  (i) Si/Mn to yield 50–70 ppm dissolved oxygen,

  (ii) Si/Mn/Al to yield 25–40 ppm dissolved oxygen,

  (iii) Si/Mn/Ca to yield 15–20 ppm dissolved oxygen.

(c) Killed steels deoxidized with aluminum to yield 2–4 ppm dissolved oxygen.

The reaction equilibrium data for steel deoxidation are discussed in depth in Chapter 2, Section 2.10. In this section the focus will be on the practical aspects of deoxidation.

11.4.1.1 Deoxidation in the Presence of Synthetic Slags

The practice of refining steel in the ladle has made it possible to deoxidize the steel partially with Fe/Mn and/or Fe/Si later followed by a final deoxidation with aluminum. Such a practice has several advantages, including minimization of nitrogen pickup during tapping as discussed in Section 11.1.1, minimization of phosphorus reversion from the carried-over furnace slag, and minimization of aluminum losses due to reaction with carried-over furnace slag.

Today the use of synthetic slags in the ladle is an integral part of ladle metallurgy because of the requirements necessary to produce ultraclean steels, frequently combined with a demand for extra low sulfur contents. The concept of using synthetic slags in ladles dates back to the 1930s when the Perrin process was developed for the enhanced deoxidation of open hearth or Bessemer steel with ferromanganese or ferrosilicon by tapping the steel on a molten calcium aluminosilicate slag placed on the bottom of the tap ladle. The dissolution of the deoxidation products such as Mn(Fe)O or manganese silicates in the calcium aluminosilicate slag lowers their thermodynamic activity, thus increasing the extent of deoxidation.

11.4.1.1.1 Partial Deoxidation with Ferromanganese Turkdogan[11] described the results obtained for deoxidation with ferromanganese in several plant trials. When deoxidizing with ferromanganese the deoxidation product is Mn(Fe)O, the activity of which is lowered in the presence of a calcium

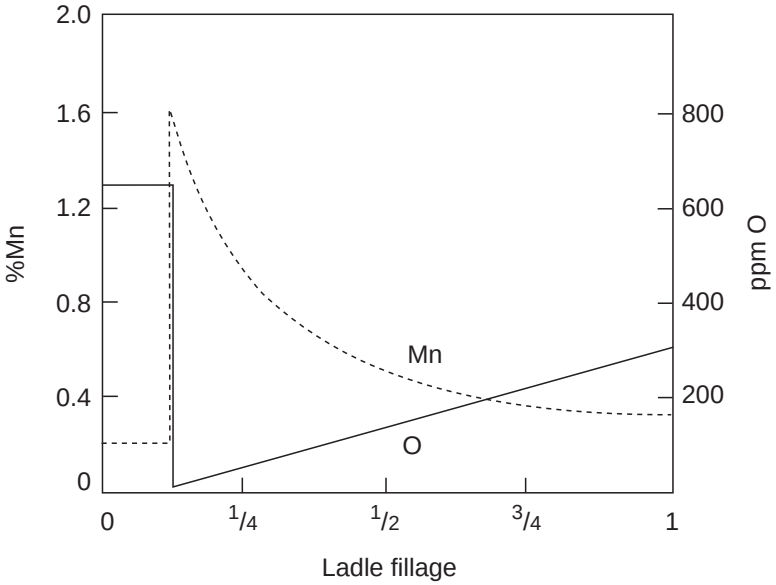

Fig. 11.15 Change in dissolved manganese and oxygen contents during tapping of a 200 tonne heat in the presence of 1800 kg ladle slag consisting of CaO-saturated calcium aluminate charged at 1/8 ladle fillage. *From Ref. 11.*

aluminate slag. The change in dissolved oxygen and manganese contents during tapping of a 200 tonne heat of steel to which 1800 kg of lime-saturated calcium aluminate and ferromanganese was added when the tap ladle was 1/8 full is shown schematically in Fig. 11.15. Upon addition of the ferromanganese, the small amount of steel present in the ladle is almost completely deoxidized, resulting in approximately 1.6% manganese in the steel. As the ladle is filled, the dissolved manganese is consumed by the deoxidation reaction and decreases to approximately 0.32% when the ladle is full and the residual dissolved oxygen content is reduced to approximately 300 ppm from the original 650 ppm at the beginning of tap.

The results obtained using this deoxidation practice in EAF and OBM (Q-BOP) shops[11] are depicted in Fig. 11.16 for steels containing less than 0.003 wt.% of aluminum and silicon each.

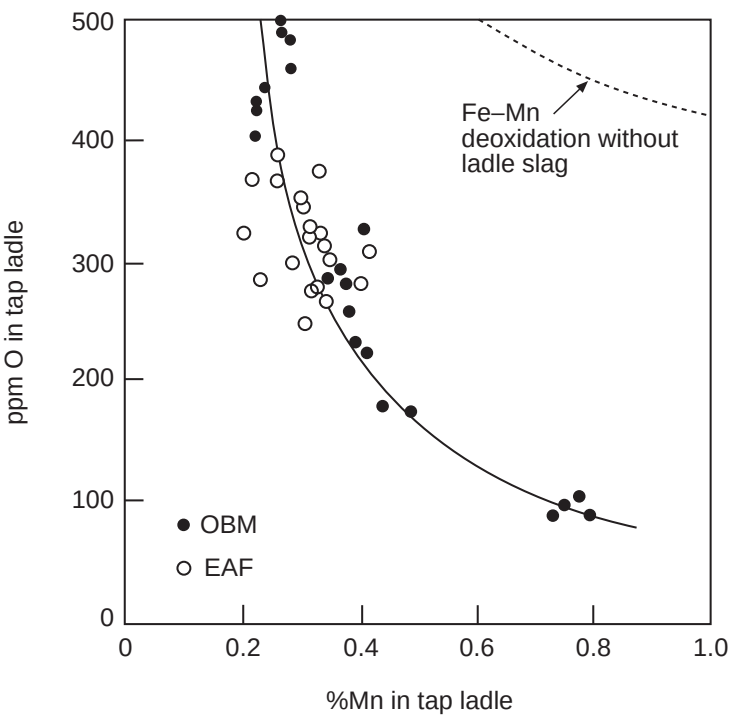

Fig. 11.16 Partial deoxidation of steel with ferromanganese and calcium aluminate slag during furnace tapping; steel containing less than 0.003% aluminum or silicon each. *From Ref. 11.*

Without calcium aluminate slag addition to the tap ladle, i.e. deoxidation with manganese and iron only and pure Mn(Fe)O as the deoxidation product, the concentration of dissolved oxygen in the steel would follow the broken line in Fig. 11.16. In the EAF trial heats there was no argon stirring in the ladle during furnace tapping. Yet, it was found that the slag-aided partial deoxidation of the steel attained during tap was close to the levels determined by the slag–metal equilibrium. This observation led Turkdogan[11] to conclude that there was sufficient mixing of slag and metal to promote relatively rapid deoxidation in the ladle during tap.

11.4.1.1.2 Deoxidation with Silicomanganese It is well known that the deoxidation of steel with manganese and silicon together leads to lower dissolved oxygen contents than the deoxidation with either of these elements alone. This is because the activities of the oxides in the deoxidation reaction

$$[Si] + 2(MnO) = 2[Mn] + (SiO_2) \qquad (11.4.1)$$

are less than unity. The symbols within the square brackets refer to species dissolved in the steel, those within parentheses to species in the manganese silicate phase. By making use of the oxide activity data in the $MnO–SiO_2$ system together with the thermodynamic data for reaction 11.4.1, Turkdogan[40] computed the equilibrium state pertaining to the deoxidation with silicomanganese, as shown in Fig. 2.127.

When the deoxidation with silicomanganese takes place in the presence of a small amount of aluminum dissolved in the steel the deoxidation product is molten manganese aluminosilicate and the resulting dissolved oxygen content is approximately 50 ppm for a steel containing roughly 0.8% manganese and 0.2% silicon.[11] This is approximately half the value in a steel deoxidized with silicomanganese and not containing aluminum. This is because the activities of MnO and SiO_2 are lowered further in the presence of the aluminosilicate phase. For example, it is possible to decrease the dissolved oxygen content to approximately 20 ppm by means of deoxidation with silicomanganese together with the addition of 1000 kg of prefused calcium aluminate to a 200 tonne heat of steel.[11]

For ladle slags containing a high percentage of alumina there will be some reduction of the alumina by the silicon in the steel. The data for steel containing aluminum and silicon in equilibrium with calcium aluminate slags containing approximately 5% silica are shown in Fig. 11.17.[2] As may be seen from this diagram, appreciable pickup of aluminum from the slag can be expected if the steel is initially low in aluminum, e.g. <0.01% Al, and contains approximately 0.2% silicon. The final stage of deoxidation of the steel in the ladle is determined by the amount of aluminum recovered from the slag.

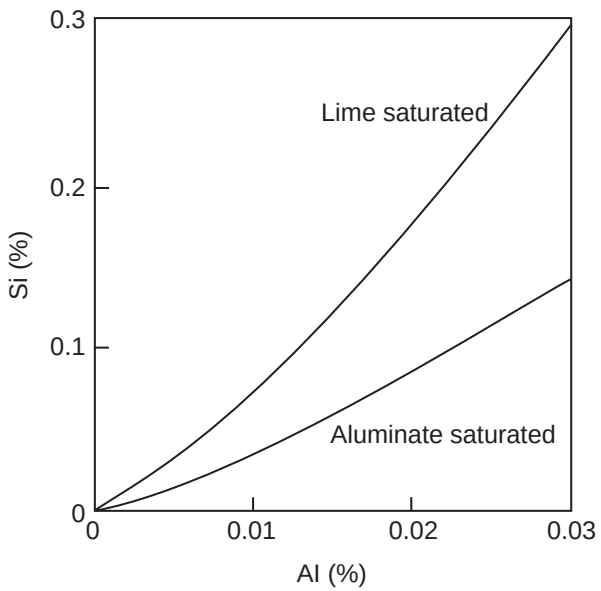

Fig. 11.17 Aluminum and silicon contents in steel in equilibrium at 1600°C with molten calcium aluminate slags containing approximately 5% SiO_2. *From Ref. 2.*

11.4.1.1.3 Deoxidation with Calcium/Silicon Semi-killed steel deoxidized with silicomanganese can be deoxidized further with calcium/silicon, e.g. by injection of Cal-Sil in the form of cored wire. Iyengar and Duderstadt[41] studied the deoxidation of 50 kg steel melts at 1620°C with silicomanganese and varying amounts of CaSi. Some of their results are shown in Fig. 11.18, from which it is seen that the dissolved oxygen content in a low carbon steel deoxidized with silicomanganese can be lowered from approximately 85 to approximately 55 ppm by adding 2.5 kg CaSi/tonne. Similar observations were made in a series of plant

trials[42] in which Cal-Sil cored wire was injected into 60 tonne heats of steel. The lower dissolved oxygen content obtained after the addition of Cal-Sil is a result of the formation of calcium manganese silicate as the deoxidation product, further decreasing the activities of MnO and SiO_2.

11.4.1.1.4 Deoxidation with Aluminum

Numerous experimental data, obtained by the emf technique, exist on the solubility product of Al_2O_3 in pure liquid iron. The reported values for 1600°C are in the range[43]

$$[\%Al]^2 \cdot [\%O]^3 = 9.77 \times 10^{-15} \text{ to } 1.2 \times 10^{-13} \quad (11.4.2)$$

The higher values are from older work when the interference with the emf readings caused by partial electronic conduction in the electrolyte of the emf cell was not well recognized. In the most recent work by Dimitrov et al.[43] the emf readings were corrected for electronic conduction, leading to the value of 9.77×10^{-15} for the Al_2O_3 solubility product at 1600°C (2912°F).

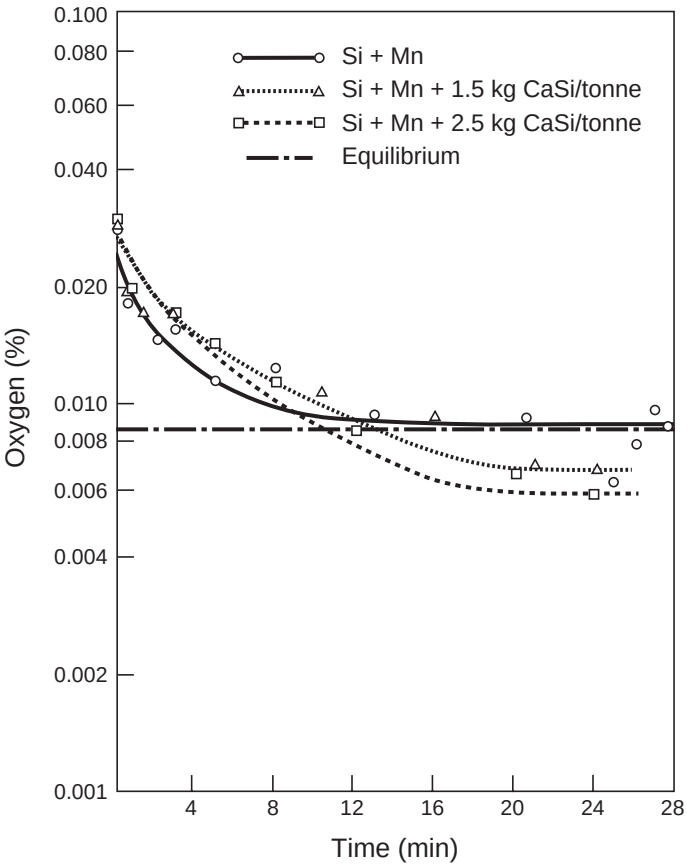

Fig. 11.18 Dissolved oxygen content in 0.05%C steel after deoxidation with SiMn and SiMn + CaSi at 1620°C; steel contained ~0.65% Mn and ~0.20% Si. *From Ref. 41.*

In addition, Dimitrov et al.[43] did a number of emf measurements in inductively stirred iron melts in contact with $CaO–Al_2O_3$ slag mixtures in which the activity of alumina was less than unity. They observed that the aluminum-oxygen relationship in these melts was indistinguishable from that in iron melts in equilibrium with pure alumina. Similar observations were reported by Schuermann et al.[44]

These experimental findings indicate that even in the presence of a calcium aluminate slag the dissolved oxygen content in steel is controlled by the alumina inclusions always present in the interior of the bath. In ladle metallurgy operations where the steel is frequently covered with a calcium aluminate slag containing minor amounts of magnesia and silica, it is therefore to be expected that the final dissolved oxygen content is controlled by the alumina inclusions dispersed throughout the bath. A measurable decrease in dissolved oxygen content as a result of treatment with calcium aluminate slag is not to be expected. A decrease in dissolved oxygen content can only be expected if substantially all the alumina inclusions have been modified to calcium aluminates, e.g. by calcium treatment; this will be discussed in more detail in Section 11.4.5.2

11.4.2 Desulfurization

In certain steel grades, such as those used in line pipe applications, a very low sulfur content is required, e.g. 20 ppm or less. These low sulfur contents can only be achieved by steel desulfurization in the ladle in the presence of a calcium aluminate slag when the steel is fully killed. Desulfurization is also discussed in depth in Chapter 2. The governing reaction is

$$\tfrac{2}{3}[Al] + [S] + (CaO) = (CaS) + \tfrac{1}{3}(Al_2O_3) \quad (11.4.3)$$

where the symbols within square brackets denote species dissolved in the steel and those within parentheses refer to species dissolved in the slag phase.

The change in free energy for reaction 11.4.3 based on the most recent data on the solubility product of alumina in liquid iron[43] is given by

$$\Delta G^\circ = -319{,}343 + 111.3T, \text{ J/mole} \tag{11.4.4}$$

This gives for the equilibrium constant of reaction 11.4.3

where

$$\left.\begin{aligned} \log K &= \frac{16{,}680}{T} - 5.813 \\ K &= \frac{a_{CaS}\; a_{Al_2O_3}^{1/3}}{a_{CaO}\; a_S\; a_{Al}^{2/3}} \end{aligned}\right\} \tag{11.4.5}$$

The oxide and sulfide activities are relative to the respective pure solid phases and the activities of aluminum and sulfur dissolved in liquid iron are defined such that for dilute solutions, below approximately 0.5 wt.%, the activities may be replaced by their respective concentrations in weight percent. For a given slag composition the activities of the oxides are fixed and may be incorporated in the equilibrium constant while the sulfur content of the slag, (%S), is proportional to the sulfide activity, a_{CaS}. Thus, the equilibrium constant may be replaced by a pseudo-equilibrium constant as follows

$$K_S = \frac{(\%S)}{[\%S]}\,[\%Al]^{-2/3} \tag{11.4.6}$$

For a given aluminum content of the steel the ratio $L_S = (\%S) / [\%S]$ is a function of the ladle slag composition at a given temperature. This is shown in Fig. 11.19 where lines of equal L_S-values are projected on the Al_2O_3–CaO–SiO_2 phase diagram for slags in equilibrium with steels containing 0.03% aluminum.[45] For different aluminum contents the L_S-values in Fig. 11.19 should be multiplied by the factor $(\%Al/0.03)^{2/3}$.

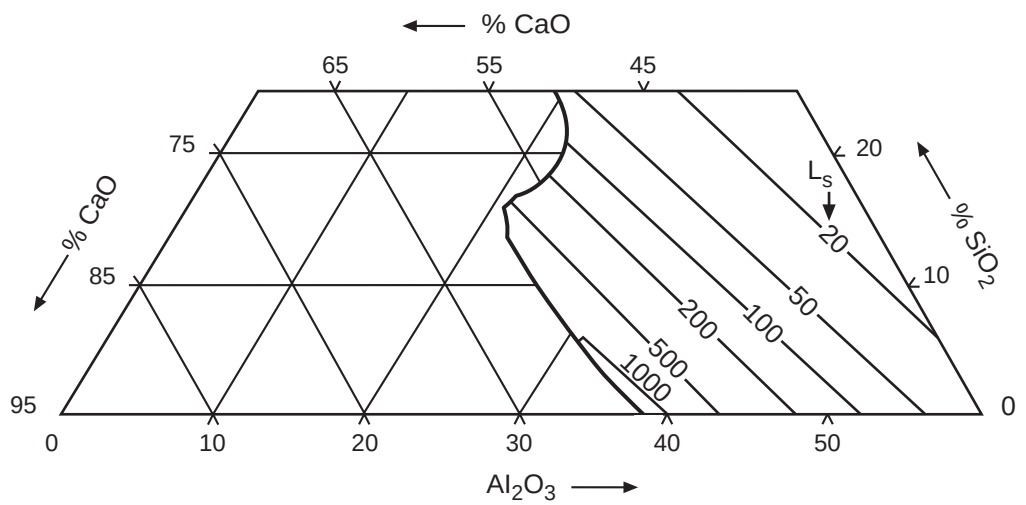

Fig. 11.19 Iso-sulfur distribution ratios for equilibria between steels containing 0.03% Al and Al_2O_3–CaO–SiO_2 slags containing 5% MgO at 1600°C. *From Ref. 45.*

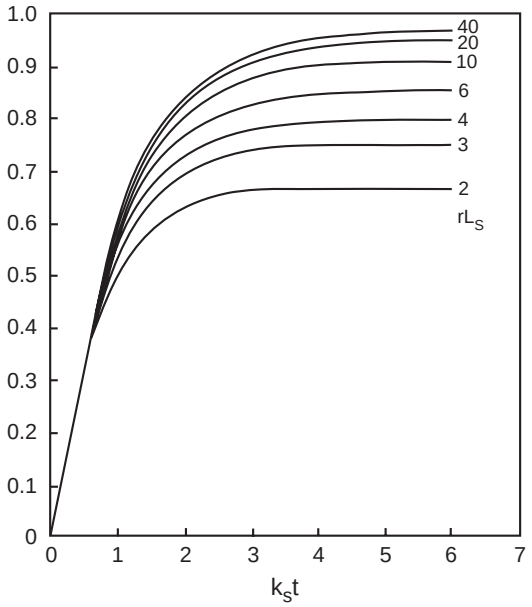

Fig. 11.20 Relative degree of desulfurization, ($R=W_s/W_m$) as affected by stirring power and time, ($k_S t$) and the product of specific quantity of ladle slag and sulfur partition ratio, (rL_S) as indicated by the numbers near the curves. *From Ref. 45.*

Depending on the specific operating conditions, the range of compositions of ladle slags commonly used is: 20–40% Al_2O_3, 35–55% CaO, 8–15% MgO and 10–15% SiO_2 together with minor amounts of FeO and MnO. In some cases CaF_2 is added to the ladle slag.

11.4.2.1 Desulfurization Rate

For reaction 11.4.3 to proceed rapidly such that the required degree of desulfurization can take place within a practical time span, good mixing of steel and slag is essential. The rate at which sulfur can be removed is, therefore, strongly affected by the gas flowrate or the stirring power density. As the capacity of typical ladle slags to absorb sulfur is high, the rate of desulfurization is controlled by mass transfer in the liquid steel and the rate of desulfurization is described by equation 2.10.19.

Riboud and Vasse[45] calculated the relative sulfur removal, R, for various conditions; the results are shown in Fig. 11.20. This diagram may be used to estimate the specific quantity of ladle slag, r, required to give the desired degree of sulfur removal, as illustrated by the following example.

Consider a shop where hard stirring, equivalent to a stirring power density of 100 W/tonne, is practiced for desulfurization with a ladle slag with a composition equivalent to L_S=500. From Fig. 11.10 the value $k_S \sim 0.13$ min^{-1} is obtained for $\dot{\varepsilon}$ = 100 W/tonne. Assume that the total time to be reserved for desulfurization is 15 min to achieve 80% desulfurization, e.g. from 0.01 to 0.002% S. From Fig. 11.20 it is found that R = 0.80 can be achieved in the given time, provided rL_S=10 or r=0.02, equivalent with a specific quantity of ladle slag of 20 kg/tonne of steel (40 lb/ton). For a stirring power density of approximately 50 W/tonne the value of k_S is estimated to be approximately 0.03 min^{-1} (Fig. 11.10) and a treatment time of 65 min would be required to achieve 80% desulfurization. This example illustrates the importance of hard stirring for effective desulfurization to low sulfur levels.

The rate of desulfurization depends on stirring rate, slag chemistry which affects L_S and Al content, which also effects L_S. Application of equation 2.10.19 indicates desulfurization equilibrium in a well-stirred ladle using 0.85–1.10 Nm^3 (30–40 scfm)Ar occurs in approximately 10–15 min.

To achieve very low sulfur contents the injection of fluxes into the ladle is often practiced. Hara et al.[46] describe results obtained by injecting 70% CaO–30% CaF_2 power mixtures into 150 tonne heats of low-carbon Al-Si killed steels. Their results are shown in Fig. 11.21. It is noted that powder injection results in a desulfurization rate that is, on average, approximately 15% faster than desulfurization with a top slag only, combined with gas stirring. This implies that the contribution of the so-called transitory reaction with the powder mixture as it ascends the bath is minor compared with the reaction with the top slag, in general agreement with a mathematical model developed by Sawada et al.[47]

Desulfurization of steel in the ladle is accompanied by a decrease in the temperature of the steel bath. Today most steelmaking shops are equipped with facilities for reheating the steel, either by electric arc or by injection of oxygen and aluminum. If no facilities for reheating are available an

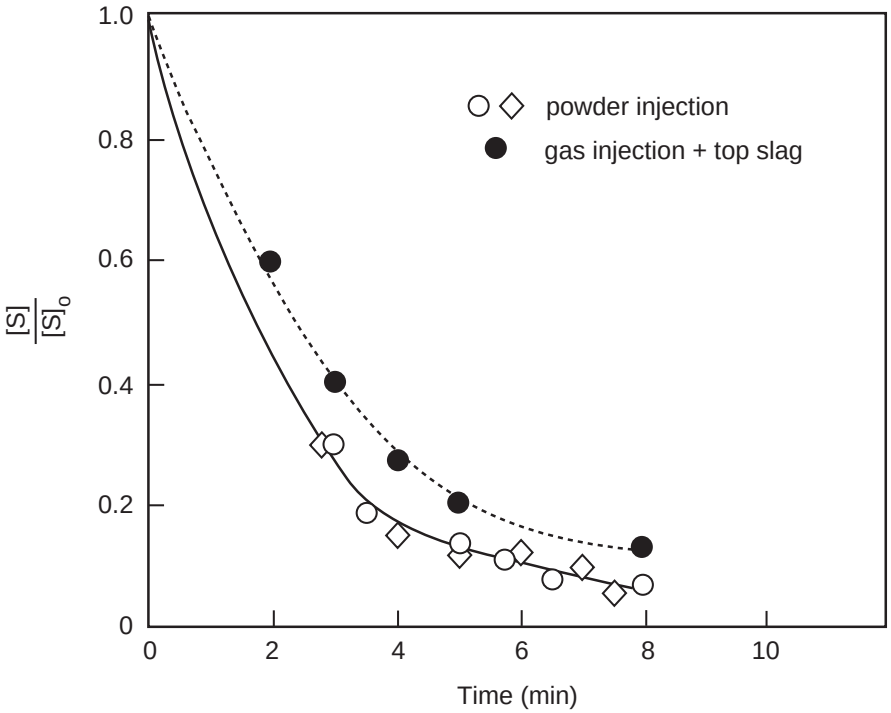

Fig. 11.21 Desulfurization of 150 tonne heats of Al-Si killed steel with mixtures of 70% CaO–30% CaF_2 (open symbols) and by gas stirring + top slag –FeO equilibrium. *From Ref. 46.*

exothermic mixture consisting of 58% burnt lime, 30% hematite and 12% aluminum powder can be used for desulfurization.[11] Further details about the use of such mixtures and the results obtained in extensive plant trials were presented by Turkdogan.[2]

11.4.3 Dephosphorization

In general it is preferred to remove phosphorus from steel under the oxidizing conditions prevalent in the BOF or in EAFs with oxygen injection. In older EAF shops equipped with furnaces with inadequate or no oxygen injection capability the need for steel dephosphorization in the ladle may

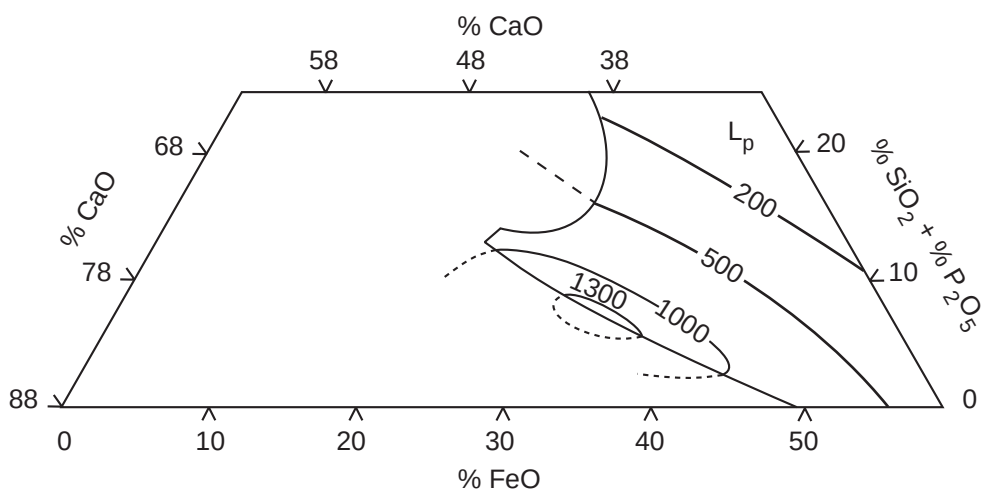

Fig. 11.22 Iso-phosphorus distribution ratios, L_P = (%P) / [%P], for equilibrium at 1600°C between steel and CaO–FeO–(SiO_2 + P_2O_5) slags containing 2% MgO, 6% MnO and 4% Na_2O; the dissolved oxygen is controlled by the Fe(filled symbols). *From Ref. 49.*

arise. Also, ladle dephosphorization may be necessary in BOF shops in which hot metal with a high phosphorus content is charged and where there is no capability of dephosphorizing the hot metal prior to charging to the BOF.

Removal of phosphorus from the steel in the ladle is achieved by treating the steel with lime-based oxidizing slags containing iron oxide. The fundamentals of the phosphorus reaction are discussed in Chapter 2.

For a steel with a given dissolved oxygen content the ratio $L_P = (\%P) / [\%P]$ is a function only of the slag composition and the temperature. This is shown in Fig. 11.22 where lines of equal L_P-values are projected on the CaO–FeO–(SiO_2 + P_2O_5) phase diagram[49], the dissolved oxygen contents being controlled by the Fe–FeO equilibrium.

Dephosphorization in the ladle during tapping of the BOF converter was studied by Becker et al.[50] who used varying quantities of a mixture of 50% CaO, 30% iron oxide (FeO_x) and 20% CaF_2. Approximately 30–40% of the mixture was placed on the bottom of the tap ladle while the remainder was added during tap. The phosphorus content of the steel tapped from the converter varied between approximately 0.01 and 0.035%. The results of these plant trials are summarized in Fig. 11.23, reproduced from the data by Becker et al.[50] It is seen from this diagram that approximately 75% of the phosphorus was removed when 12 kg/tonne of the aforementioned mixture was used. In the practice described by Becker et al.[50] the high-phosphorus slag was removed by reladling followed by reheating in a ladle furnace.

Another example of steel dephosphorization in the ladle at tap is given by Bannenberg and Lachmund.[51] In this practice the steel was tapped open while, depending on the anticipated quantity of converter slag carryover, varying amounts of lime, ore and sometimes fluorspar were added during tap to produce a lime-saturated dephosphorizing slag high in iron oxide. The results of these trials indicate 60–70% phosphorous removal.

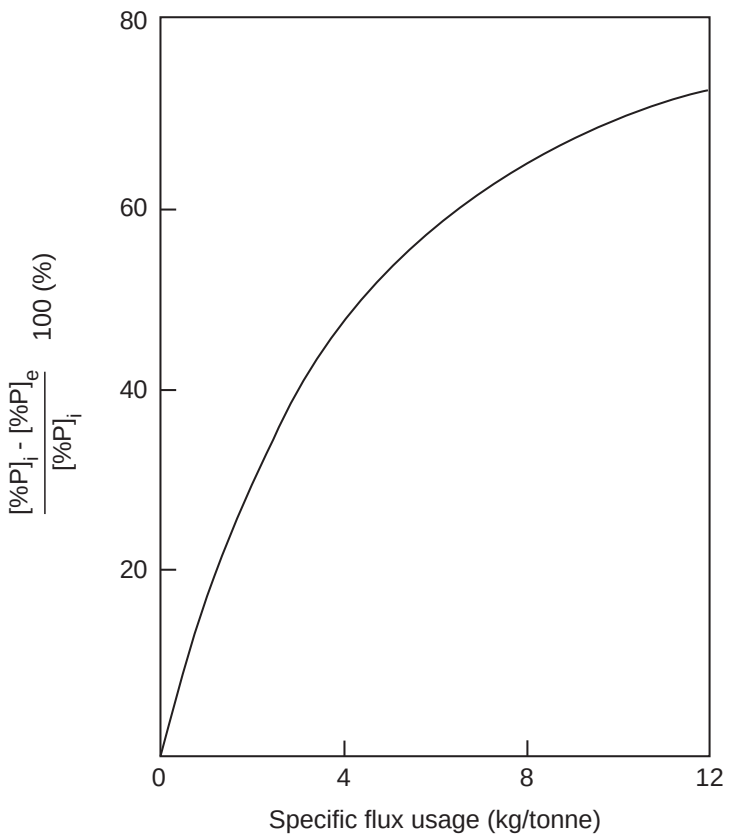

Fig. 11.23 Degree of dephosphorization during tap as affected by the specific quantity of 50% CaO–30% FeO_X–20%CaF_2 used, reproduced from data by Becker et al.[50]

Because of the oxidizing conditions prevailing during dephosphorization, manganese and chromium losses are to be expected, as discussed by Bannenberg and Lachmund.[51] The authors derived the following relationship between the loss in chromium or manganese, η_X, and the degree of dephosphorization, η_P

$$\eta_X = \frac{100\ \eta_P}{100\ K_X - \eta_P(K_X - 1)} \tag{11.4.7}$$

where

X = Cr or Mn and
η_X = $\{[\%X]_i - [\%X]_f\} / [\%X]_i$
η_P = $\{[\%P]_i - [\%P]_f\} / [\%P]_i$

From the plant data Bannenberg and Lachmund[51] derived the following values for K_X: $K_{Cr} = 6.6$ and $K_{Mn} = 2.2$. For example, for 50% phosphorus removal ($\eta_P = 50$) the chromium loss would be 13% ($\eta_{Cr} = 13$) while the manganese loss would be 31% ($\eta_{Mn} = 31$), as found from equation 11.4.7.

11.4.4 Alloy Additions

Metals and alloys can be added to liquid steel at various stages in the steelmaking process, e.g. inside the furnace, during furnace tapping, in the ladle furnace, during vacuum treatment, etc. The timing of the additions depends on the process route, the shop logistics and on certain characteristics of the addition in question such as its melting point, volatility and its susceptibility to oxidation. For example, nickel can be added to the EAF at any time as nickel oxide, which is easily reduced. In the oxygen steelmaking process route alloying additions such as ferrosilicon and ferromanganese are made during furnace tapping while the other alloys are added in subsequent stages of secondary steelmaking.

Argyropoulos and Guthrie[53] were perhaps the first to undertake a systematic study on the dissolution kinetics of ferroalloys. They defined two broad categories of ferroalloys: class I ferroalloys with melting points below the temperature of liquid steel, and class II ferroalloys with melting points higher than the liquid steel temperature. The thermophysical properties of the class I and class II ferroalloys are summarized in Tables 11.5 and 11.6, respectively.

When a ferroalloy is added to liquid steel a solidified shell of steel forms around the alloy particle as a result of the local chilling effect. As time progresses, the shell melts while the ferroalloy inside the shell is heated to its melting point. The complete dissolution is governed by convective heat transfer processes in the bath as well as the size of the ferroalloy added.

The class II ferroalloys, listed in Table 11.6 all have melting points higher than the temperature of the liquid steel. These alloys dissolve at a slower rate than the class I alloys, their dissolution rate being controlled by mass transfer in the liquid steel, even in agitated baths. It is, therefore, important to ensure that their size is within 3–10 mm in order to obtain good mixing, fast dissolution and high recovery rates. Compacted powder mixtures of ferroalloys such as ferrovanadium, ferrotungsten and ferromolybdenum dissolve faster than solid pieces of similar size. Autoexothermic alloys, which generate heat upon melting, can also be used for faster melting and dissolution as well as improved recovery. Argyropoulos and Guthrie[53] present a number of predicted dissolution times for an assortment of ferroalloys of varying sizes under a number of different conditions such as bath temperature and convection within the bath.

In a later investigation Lee et al.[54] made an extensive study of the dissolution kinetics in liquid steel as well as in slags of the most widely used ferroalloys such as ferrosilicon (75 FeSi), silicomanganese (SiMn), high-carbon ferromanganese (HCFeMn) and high-carbon ferrochrome (HCFeCr). Their findings corroborated the earlier results of Argyropoulos and Guthrie.[53]

Table 11.5 Physical and Thermal Properties Relevant to Class I Ferroalloys.
From Ref. 53.

Material	Density kg m^{-3}	Heat Capacity J kg^{-1} K^{-1}	Thermal Conductivity W m^{-1} K^{-1}	Latent Heat kJ kg K^{-1}	$T_{solidus}$ K	$T_{liquidus}$ K
Ferromanganese Mn = 79.5% C = 6.4% Si = 0.27% Fe: balance	7200	700.0	7.53	534,654	1344	1539
Silicomanganese Mn = 65.96% Si = 17.07% C = 1.96% Fe: balance	5600	628.0	6.28	578,783	1361	1489
50% Ferrosilicon Si = 49.03% Al = 1.20% max Fe: balance	4460	586.0	9.62	908,200	1483	1500
Ferrochrome Cr = 50–58% C = 0.25% max Si = 1.5% max Mn = 0.50% max Al = 1.50% max	6860	670.0	6.50	324,518	1677	1755

Table 11.6 Physical and Thermal Properties Relevant to Class II Ferroalloys.
From Ref. 53.

Material, A.	Density kg m^{-3} (1873K)	Heat Capacity J kg^{-1} K^{-1}	Thermal Conductivity W $m^{-1}K^{-1}$	Diffusivity $D_{A/Fe} \times 10^9$ m^{2-1}
Molybdenum	10000	310.0	100.0	3.2
Vanadium	5700	400.0	50.0	4.1
Niobium	8600	290.0	64.0	4.6
Tungsten	19300	140.0	115.0	5.9

Several methods of alloy addition are practiced. Examples are: throwing of filled bags, adding with a shovel or via mechanized chutes, wire feeding, powder injection, bullet shooting, etc. A special process for making alloy additions is the so-called CAS process (Composition Adjustment by Sealed argon bubbling). In this process a refractory-lined snorkel is partially immersed in the steel bath in such a manner that it envelopes the ascending gas plume created by the injection of argon through the porous plug in the ladle bottom. Alloy additions are made onto the liquid steel surface within the area covered by the snorkel. The plume eye within the snorkel is filled with argon, thus has a low oxygen partial pressure preventing oxidation of the alloy addition. Melting and distribution rates are

high as a result of the agitation brought about by the ascending gas bubbles. Mazumdar and Guthrie[55] have made water model studies to investigate the subsurface motion of both buoyant and sinking additions in the CAS process. The study showed that buoyant additions such as aluminum and ferrosilicon dissolve more readily into the steel bath rather than react partially with the slag as in conventional addition methods, thus giving improved recovery. The authors further recommend that ferromanganese and ferroniobium be crushed to an average size of approximately 5 mm to obtain better control.

Wirefeeding of alloys by means of the cored-wire techniques, developed primarily for the addition of calcium to steel, is practiced for adding elements that are less dense than steel or have a limited solubility, high vapor pressure and high affinity for oxygen. Wirefeeding is also used in cases where the element to be added is toxic or when very small additions are required. The cored-wire technique permits the quantity of alloy or elements being fed into the steel to be adjusted with high precision and to trim the composition of the steel within narrow limits. For example, ferroboron or tellurium additions can be made in precise and minute quantities by wirefeeding. Excessive additions of these elements may cause hot-shortness.

It is also possible to wirefeed aluminum with the same wirefeeding equipment used for cored-wire. Advantages of aluminum wire additions include: higher recovery, better control of aluminum content, and improved cleanliness.[56] Herbert et al.[57] give examples of improved control of the steel aluminum content by wirefeeding at the Lackenby plant of the British Steel Corporation.

Schade et al.[58] studied the dissolution characteristics of cored-wire additions of ferromolybdenum, ferroniobium and ferrochromium modified with minor quantities of silicon—so-called microexothermic alloys—to achieve improved dissolution into liquid steels. The exothermicity exhibited by these modified alloys is based on the formation of an intermetallic compound (a silicide) which is accompanied by the release of heat. The enthalpy released is sufficient to melt the compound, thus allowing rapid dissolution of the ferroalloy into the liquid steel. The enhanced dissolution rate of these modified ferroalloys makes them well-suited for tundish additions where the relatively short residence time requires a rapid dissolution of additions.

11.4.5 Calcium Treatment and Inclusion Modification

The addition of calcium to steel goes back a long time, Watts[59] being the first to add CaSi to a steel melt. The widespread practice of calcium additions to steel melts did not start until the 1960s with the development of improved addition methods and composite calcium-bearing alloys. Today calcium

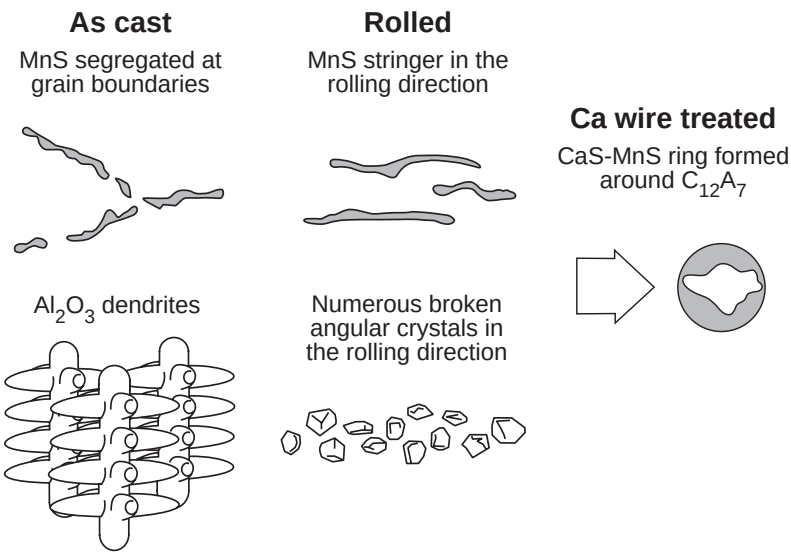

Fig. 11.24 Schematic illustration of modification of inclusion morphology as a result of calcium treatment. *From Ref. 2.*

treatment of steel is a common practice, with particular emphasis on the modification of alumina inclusions in aluminum-killed steels to prevent nozzle clogging during continuous casting operations.

As a result of the treatment with calcium, the alumina and silica inclusions are converted to liquid calcium aluminates or calcium silicates. These liquid inclusions are globular in shape because of surface tension effects. This change in inclusion composition and shape is commonly known as inclusion morphology control or modification. The effect of calcium treatment on inclusion morphology is illustrated schematically in Fig. 11.24.

It is seen from Fig. 11.24 that few or no sulfide stringers are expected to be present after rolling steel that was successfully treated with calcium. This phenomenon is known as sulfide shape control by calcium treatment, the underlying fundamental principles of which will be discussed later.

Examples of other metallurgical advantages brought about by the modification of oxide and sulfide inclusions by calcium treatment of steel are:[2] improvement of castability in continuous casting operations through minimization or prevention of nozzle clogging; decreasing inclusion-related surface defects in billet, bloom and slab castings; improving the machinability of the final product at high cutting speeds; and minimization of the susceptibility of high-strength low-alloy (HSLA) line pipe steels to hydrogen-induced cracking (HIC) in sour gas or oil environments.

11.4.5.1 Addition of Calcium to Steel Melts

The boiling point of calcium is 1491°C (2716°F), accordingly calcium is a vapor at steelmaking temperatures. Thus, when adding calcium to liquid steel special measures must be taken to ensure its proper recovery in the steel bath. Recently developed processes for adding calcium to a liquid steel bath are all based on the principle of introducing the calcium or calcium alloy into the bath at the greatest possible depth so as to make use of the increased pressure from the ferrostatic head to prevent the calcium from evaporating.

Ototani[60] gives details regarding the TN (Thyssen Niederrhein) process for injecting calcium with argon as a carrier gas as well as the SCAT process, also known as the bullet shooting method. Today the majority of the steel producers add calcium by wirefeeding. The principle is similar to wirefeeding of ferroalloys and aluminum, discussed in Section 11.4.4.

When wirefeeding calcium in the conventional manner, there is a possibility that the wire does not travel in a straight downward line after entering the bath, thus causing the calcium to be released at a shallow bath depth and decreasing the calcium recovery in the steel. To prevent this, the so-called wire lance (WL) method for adding calcium was developed. A schematic illustration is depicted in Fig. 11.25.

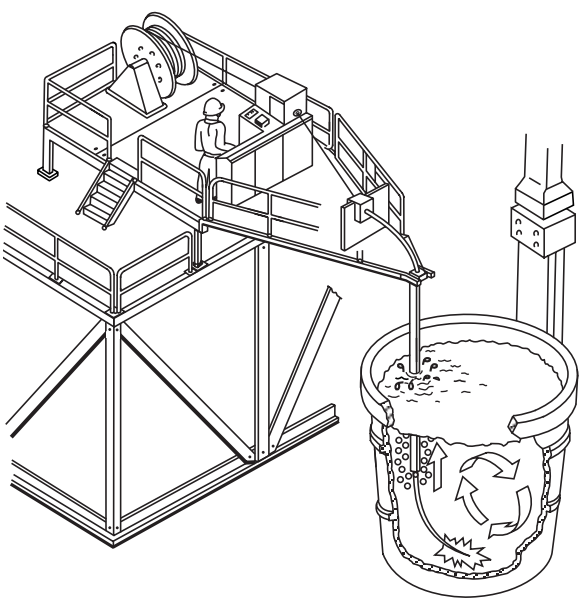

Fig. 11.25 Wire lance method for adding calcium in which calcium wire is fed through a refractory lance immersed in the bath with argon flowing through the lance during wirefeeding. *From Ref. 60.*

The wire lance method ensures that the calcium wire travels in a straight downward line after entering the bath while it is claimed that the dispersion of calcium throughout the bath is improved by the argon which is injected simultaneously. The calcium recovery or yield observed for additions with the wire lance process is compared with that observed for conventional wirefeeding in Fig. 11.26. The better recovery of calcium obtained with the wire lance method is especially pronounced for calcium addition rates less than approximately 0.2 kg/tonne (0.4 lb/ton).

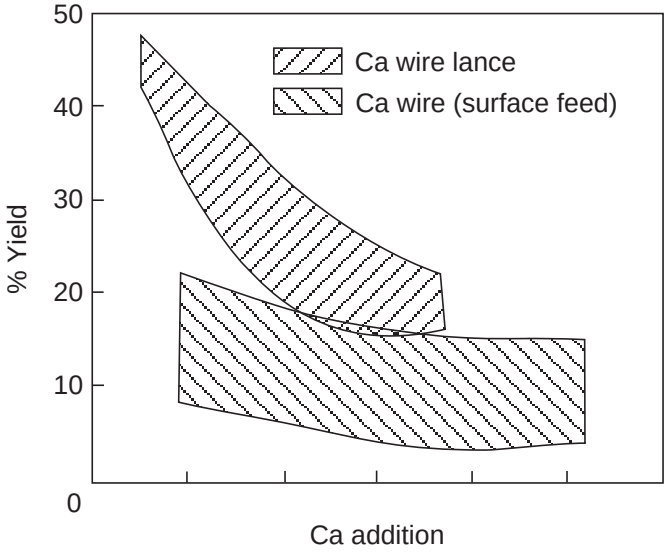

Fig. 11.26 Comparison of calcium recoveries (yields) obtained with the wire lance addition method and those obtained with conventional wirefeeding. *From Ref. 60.*

11.4.5.1.1 Calcium Usage Efficiency

The material balance for calcium consumption is expressed as follows

$$W_i = W_b + W_o + W_o' + W_s + W_v \tag{11.4.8}$$

where

W_i = amount of calcium injected,

W_b = amount of calcium dissolved in the bath,

W_o = amount of calcium present in aluminates and sulfides,

W_o' = amount of calcium reacted with alumina and subsequently floated out,

W_s = amount of calcium reacted with the slag,

W_v = amount of calcium escaped via the vapor phase and subsequently burnt at the bath surface.

It is generally accepted[2] that $W_b << W_o$, thus giving for the efficiency of calcium usage

$$\eta\,(Ca)_u = \frac{W_o + W_o'}{W_i} * 100\% \tag{11.4.9}$$

while the efficiency of calcium retention in the steel is given by

$$\eta\,(Ca)_r = \frac{W_o}{W_i} * 100\% \tag{11.4.10}$$

Experience obtained in numerous plant trials has shown that the calcium retention efficiency decreases with increasing quantity of calcium injected. The amount of calcium to be injected has to be adjusted in accordance with the degree of cleanliness of the steel or its total oxygen content. Obviously, injecting more calcium than can react with the available inclusions leads to a low calcium retention efficiency. Furthermore, it is to be expected that the calcium retention efficiency in

the continuous casting mold or in the teeming ingot will be lower than the retention efficiency in the ladle because of flotation of calcium-containing inclusions out of the bath in the time interval prior to casting or teeming. Turkdogan[2] quotes the following calcium retention efficiencies in the ladle and the tundish for aluminum-killed steels initially containing 50 to 80 ppm oxygen as alumina inclusions

Ca injected (kg/tonne)	Ladle $\eta\ (Ca)_r$	Tundish $\eta\ (Ca)_r$
0.16	24–30%	12–15%
0.36	12–18%	6–9%

11.4.5.2 Reactions of Calcium in Steel and Inclusion Modification

Regardless of the form in which calcium is added to liquid steel, e.g. as Cal-Sil, Ca-Al or as pure calcium admixed with nickel or iron powder, the subsequent reactions taking place in the bath are the same. The following series of reactions is expected to occur to varying extents in aluminum-killed steels containing alumina inclusions and sulfur

$$Ca\ (l) \rightarrow Ca\ (g) \tag{11.4.11}$$

$$Ca\ (g) \rightarrow [Ca] \tag{11.4.12}$$

$$[Ca] + [O] \rightarrow CaO \tag{11.4.13}$$

$$[Ca] + [S] \rightarrow CaS \tag{11.4.14}$$

$$[Ca] + (x + 1/3)Al_2O_3 \rightarrow CaO\bullet\ xAl_2O_3 + 2/3[Al] \tag{11.4.15}$$

$$(CaO) + 2/3[Al] + [S] \rightarrow (CaS) + 1/3(Al_2O_3) \tag{11.4.16}$$

The symbols within square brackets refer to species dissolved in the steel, those within parentheses are dissolved in the aluminate phase.

Observations by a number of investigators have indicated that the extent to which reaction 11.4.13 occurs is negligible. For steels with sufficiently low sulfur contents reaction 11.4.15 will take place first, followed by reaction 11.4.16. The critical question is for which sulfur content reaction 11.4.14 predominates such that, for a given quantity of calcium added, there is insufficient calcium available to modify the alumina inclusions according to reaction 11.4.15. Adequate modification of the solid alumina inclusions into liquid calcium aluminates is essential in order to prevent nozzle clogging during continuous casting operations.

By combining the data for the activities of the oxides in aluminate melts[61,62] with the equilibrium constant for reaction 11.4.16 as given by equation 11.4.5, the critical sulfur content for the formation of liquid calcium aluminates can be evaluated.[63] The results are shown in Fig. 11.27 and Fig. 11.28 where the critical sulfur and aluminum contents for the formation of liquid alumina-saturated calcium aluminate and liquid $12CaO\bullet7Al_2O_3$ are shown.

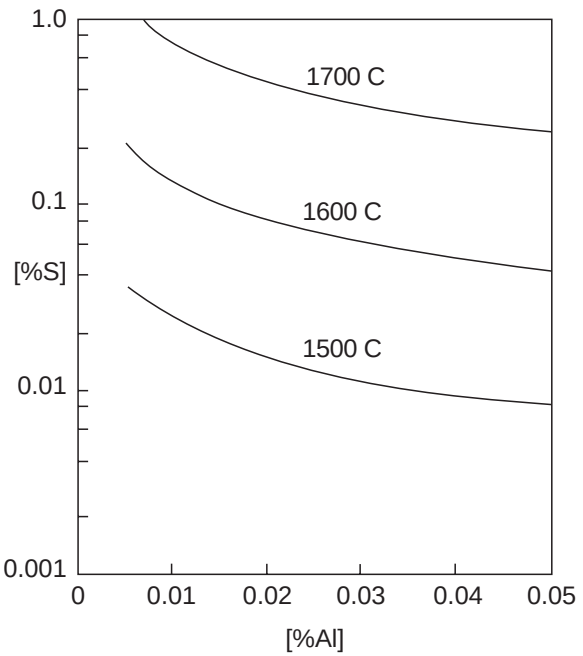

Fig. 11.27 Critical steel sulfur and aluminum contents below which liquid alumina-saturated calcium aluminate is formed at the indicated temperatures; $a_{CaS} = 1$. *From Ref. 63.*

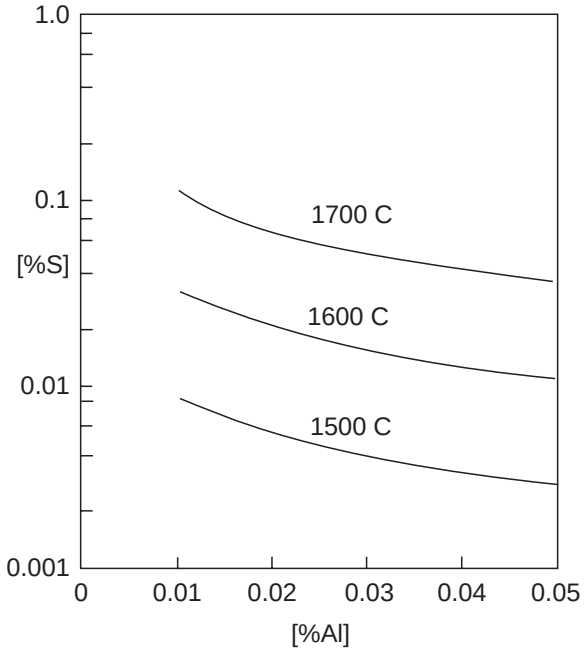

Fig. 11.28 Critical steel sulfur and aluminum contents below which liquid $12Ca•7Al_2O_3$ is formed at the indicated temperatures; $a_{CaS} = 1$. *From Ref. 63.*

Whenever the aluminum and sulfur contents in the steel fall below a curve for a given temperature, the formation of a liquid calcium aluminate is favored.

The underlying assumption made in the calculations of the diagrams in Fig. 11.27 and Fig. 11.28 was that the activity of calcium sulfide equals unity. However, the presence of manganese in most steels causes the sulfur to precipitate as calcium manganese sulfides, Ca(Mn)S, in which the activity of calcium sulfide in less than unity, thus decreasing the critical sulfur content for the formation of liquid calcium aluminate. Kor[63] has shown that the presence of up to 2% manganese in the steel has only a small effect on the critical sulfur content. The relationship between aluminum and sulfur for the formation of liquid calcium aluminates for $a_{CaS} = 0.75$ is shown in Fig. 2.139.

Larsen and Fruehan[64] studied the modification of oxide inclusions by calcium in a number of samples obtained from laboratory melts as well as from steelmaking operations. The results from this study are summarized in Fig. 11.29 from which it may be seen that the agreement with the theoretical predictions, indicated by the curves labeled CA and $C_{12}A_7$, is generally good.

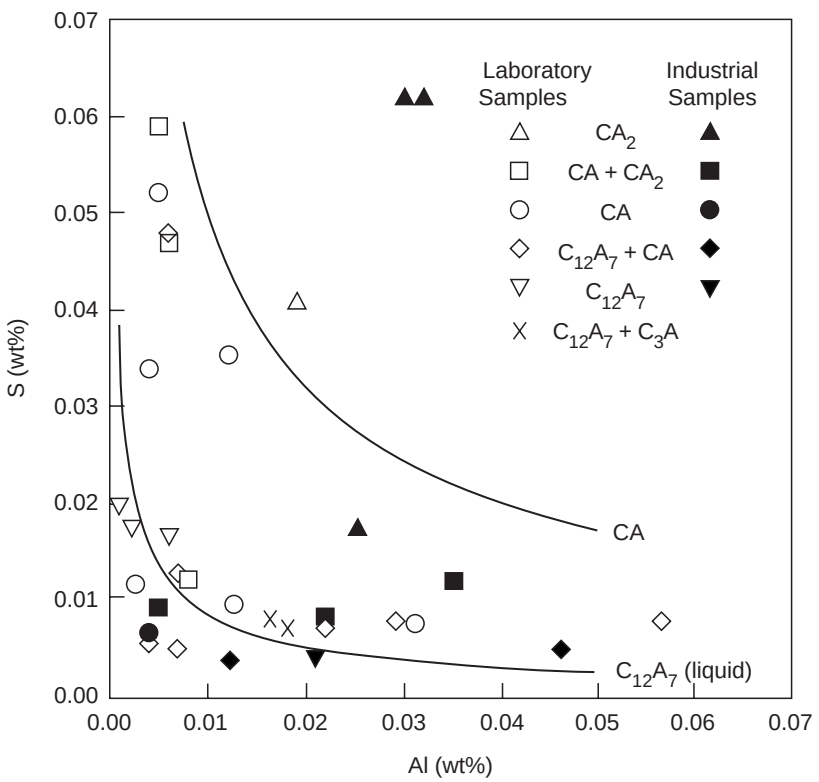

Fig. 11.29 Composition of inclusions found in laboratory and plant samples compared with theoretical predictions. *From Ref. 64.*

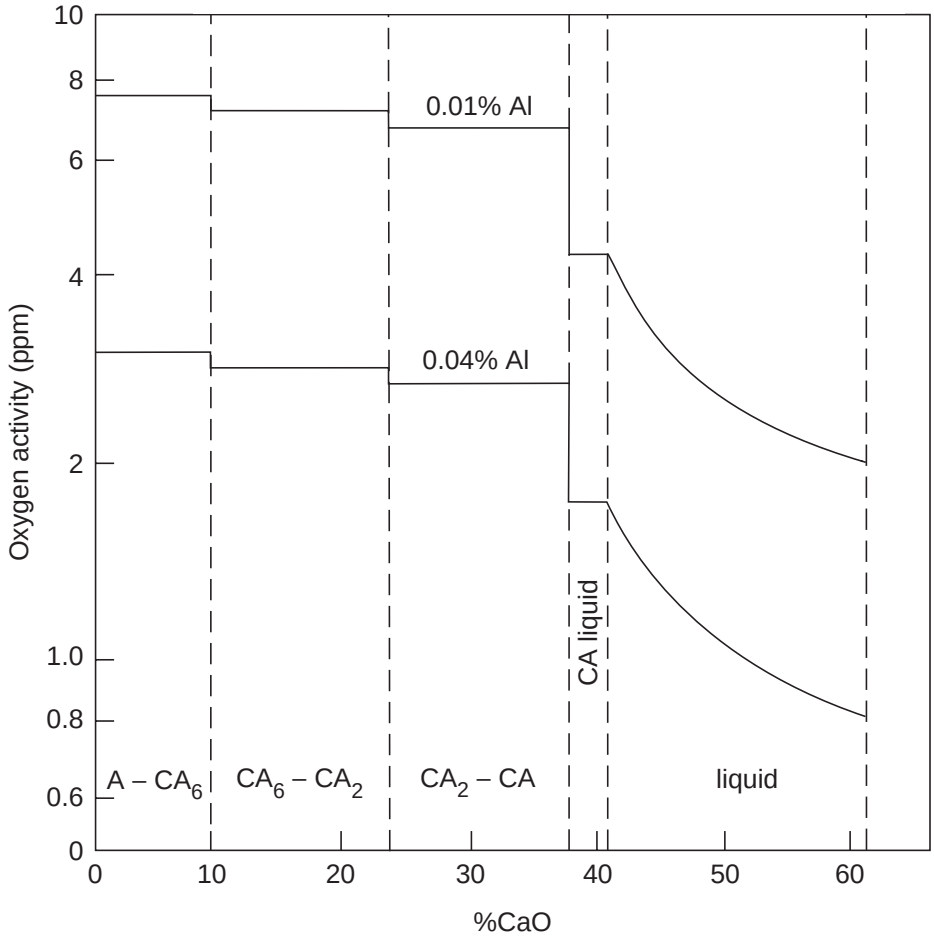

Fig. 11.30 Calculated oxygen activity in steels containing 0.01 and 0.04% Al in equilibrium with the indicated calcium aluminate at 1600°C. *From Ref. 64.*

In general, it is difficult to assess whether the injection of calcium into the steel has resulted in the desired degree of inclusion modification. Larsen and Fruehan[64] have pointed out that, in theory, the degree of inclusion modification can be determined by measuring the activity of oxygen in the steel by means of an oxygen sensor. In general, the activity of alumina in calcium aluminate inclusions is less than unity. Thus, the activity of oxygen in a steel in equilibrium with a calcium aluminate is less than that in a steel in equilibrium with alumina. As the inclusions are modified from alumina to calcium-rich calcium aluminate, the activity of oxygen in the steel decreases, provided the aluminum content of the steel is essentially constant. This is shown schematically in Fig. 11.30 from which it can be seen that the decrease in oxygen activity (in ppm) is significant whenever complete modification to liquid calcium aluminate has occurred. Thus, an oxygen sensor measurement before and after calcium treatment should, in principle, indicate how effective the treatment was in terms of inclusion modification.

In many samples obtained from steelmaking operations the oxide inclusions contain varying amounts of magnesia. Kor[63] has estimated the effect of the presence of magnesia in the oxide inclusions on the critical sulfur content for the formation of liquid calcium magnesium aluminate inclusions for a given aluminum content of the steel. It was found that for inclusions containing less than 10% magnesia, the critical sulfur content is somewhat higher than that for inclusions not containing magnesia.

11.4.5.3 Sulfide Shape Control

In steels not treated with calcium, the sulfur precipitates as finely dispersed manganese sulfide particles in the interdendritic liquid that freezes last. The manganese sulfides delineate the prior austenitic grain boundaries in the as-cast structure. During hot rolling the manganese sulfide particles are deformed, resulting in stringers in the rolled product. These stringers make the final product susceptible to, for example, hydrogen-induced cracking in sour gas or oil environments.

In calcium-treated low-sulfur steels the grain boundary precipitation of MnS during solidification is suppressed as a result of the precipitation of sulfur as a Ca(Mn)S complex on the calcium aluminate inclusions as indicated by the following reaction

$$(CaO) + 2[S] + [Mn] + 2/3[Al] \rightarrow (CaS{\bullet}MnS) + 1/3(Al_2O_3) \qquad (11.4.17)$$

The extent of sulfide shape control that can be achieved during solidification of calcium-treated steel depends on the total oxygen, sulfur and calcium contents of the steel. This is described by a model based on the reactions occurring in the impurity enriched interdendritic liquid during solidification.[65] On the basis of this model, the following criteria can be derived for the tundish compositions of aluminum-killed steels to give adequate sulfide shape control in the final product.[2]

Table 11.7 Tundish Composition Ranges for Al-Killed Steels to Achieve Acceptable Sulfide Shape Control. *From Ref. 2.*

O (ppm) as aluminate inclusions	Ca (ppm)	Mn (%)	S (ppm)
25	20–30	0.4–0.6	<20
25	20–30	1.3–1.5	<30
12	15–20	0.4–0.6	<10
12	15–20	1.3–1.5	<15

In steels with a total oxygen content of 10 ppm or less and relatively high sulfur contents, e.g. > 100 ppm, sulfide shape control by means of calcium treatment is obviously not feasible. To minimize the occurrence of sulfide stringers in such steels, the addition of tellurium or sometimes selenium has been found to be beneficial. Due to the strong effect of both these elements on the interfacial tension between sulfides and steel, the tendency of sulfide stringer formation during rolling is decreased. The result is that after rolling the sulfides are ellipsoidal in shape with a length-to-width ratio that depends on the Te/S-ratio in the steel.[63] Tellurium is usually added to liquid steel either by powder injection or by wirefeeding.

11.5 Vacuum Degassing

Vacuum degassing of steel has an even longer history than the treatment of steel with calcium, Aitken[66] possibly being the first to have proposed an arrangement for the ladle degassing of a heat of steel. An overview of the various processes in use until 1965 was given by Flux.[67] Since the 1950s and 1960s many new developments have taken place in regard to equipment for the vacuum treatment of steel as well as the technology of steel refining in vacuum degassing facilities. A more recent overview dealing with vacuum degassing was prepared by Fruehan.[68]

Initially, vacuum degassing was used primarily for hydrogen removal. However, during the last twenty years or so there has been an increased use of vacuum degassing for the production of ultra-low-carbon (ULC) steels with carbon contents of 30 ppm or less. Furthermore, a relatively new family of steel grades, the so-called interstitial-free (IF) steels with carbon and nitrogen contents of 30 ppm or less, has appeared on the scene. To achieve these low carbon and nitrogen contents,

a treatment under vacuum is mandatory. Presently, almost every high-quality steel producer has installed a vacuum treatment facility.

11.5.1 General Process Descriptions

More detailed schematic illustrations of the most popular degassing systems are presented in Section 11.6. For the purpose of the present discussion a brief description of the salient features is given here. There are two principal types of degassers: recirculating systems such as RH, RH-OB, RH-KTB and DH; and non-recirculating systems such as ladle or tank degassers, including VAD (vacuum arc degassing) and VOD (vacuum oxygen decarburization), and stream degassers.

In both recirculating and non-recirculating systems argon is used as the lifting or stirring gas. In recirculating systems the argon is used as the so-called lifting gas to lower the apparent density of the liquid steel to be lifted up from the ladle into the vacuum vessel. In non-recirculating systems argon is used as the stirring gas to promote the removal of hydrogen and/or nitrogen and to homogenize the bath.

The decision which degassing system, recirculating or non-recirculating, to install in a given shop is largely determined by the product mix to be produced. If a relatively large number of heats has to be decarburized to very low levels to produce ULC or IF steels, a recirculating system such as the RH or one of its modifications is usually preferred. For example, a carbon content of 25 ppm can easily be attained in an RH or RH-OB (KTB) degasser whereas in a tank degasser, such as a VOD, such low carbon contents cannot be attained within a practical time span.

As will be discussed later, there is not much difference between recirculating and non-recirculating systems in terms of the effectiveness with which hydrogen or nitrogen can be removed. Thus, if the primary function of the degasser is to remove hydrogen and sometimes nitrogen, the choice of system will be determined primarily by the desired match between the steel melting vessel (BOF or EAF) and the caster as well as by considerations in regard to capital and operating costs.

11.5.2 Vacuum Carbon Deoxidation

One of the purposes to treat steel in an RH or RH-OB (KTB) degasser is to lower the dissolved oxygen content of the steel by means of carbon deoxidation before adding aluminum to kill the steel completely. With such a carbon deoxidation practice there are considerable cost savings as a result of the decreased usage of aluminum.

Vacuum carbon deoxidation is described by the following reaction

$$[C] + [O] \rightarrow CO\ (g) \qquad (11.5.1)$$

where the carbon and oxygen are dissolved in the steel bath. The carbon-oxygen relationship during the vacuum decarburization treatment is schematically illustrated in Fig. 2.138. In the RH process, decarburization proceeds nearly to the stoichiometrically related decrease in carbon and oxygen contents:Δ ([O] = (16/12) Δ[C]. This is also called the self-decarburization process.

Because in the RH-OB (KTB) process oxygen is supplied from an outside source, decarburization initially takes place without a simultaneous decrease in the steel oxygen content, the so-called forced decarburization. In the later stages decarburization follows the path of self-decarburization. One of the advantages of an RH-OB (KTB) over a conventional RH is that the steel can be tapped at a higher carbon content, thus decreasing converter processing time and increasing the iron yield (lower slag FeO).

Plant data obtained for the carbon and oxygen contents of the steel before and after RH treatment are shown in Fig. 11.31, reproduced from data quoted by Turkdogan.[2] Similar results are obtained with the tank degasser.[69] Although the pressure in the vacuum vessel was approximately 0.001 atm, the final carbon and oxygen contents correspond to CO pressures varying from 0.06 to 0.08 atm, Fig. 11.31.

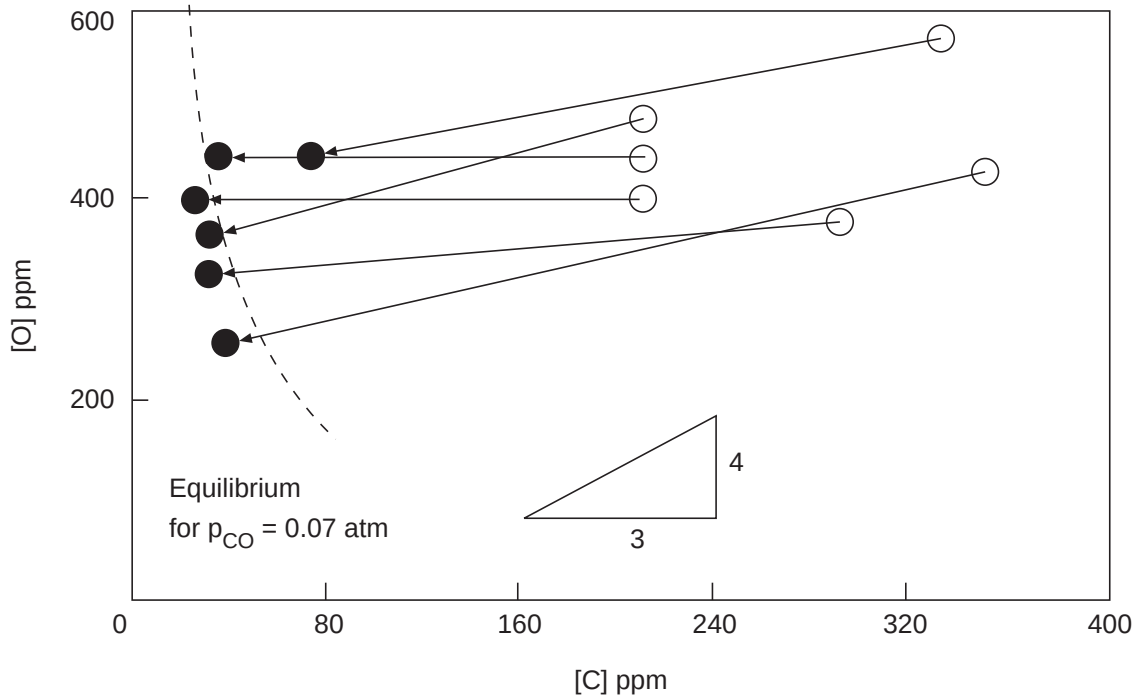

Fig 11.31 Carbon and oxygen contents of steel before (open symbols) and after (filled symbols) RH treatment, from data reported by Turkdogan.[2]

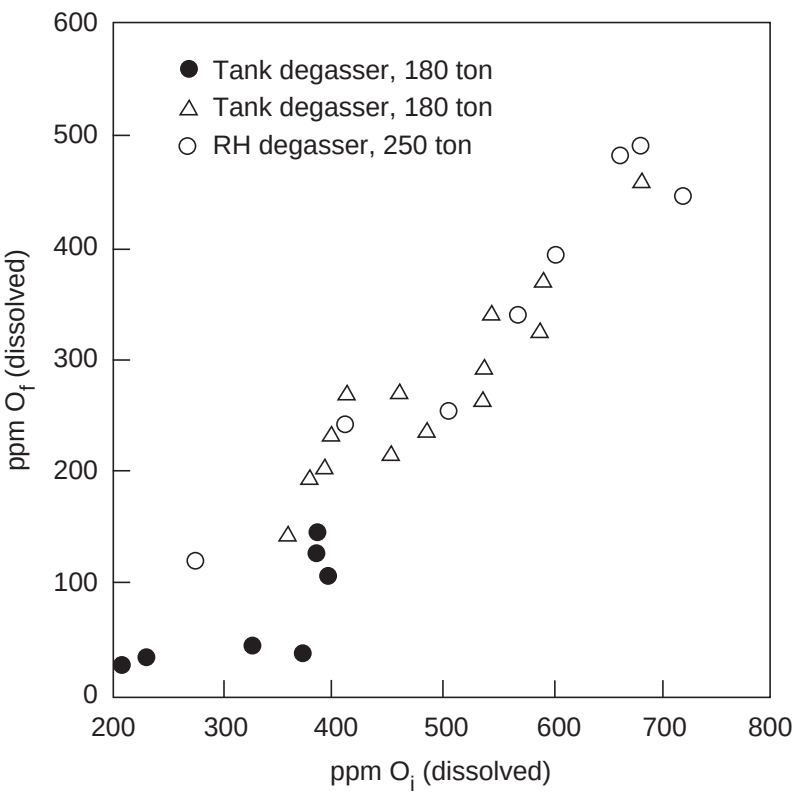

Fig. 11.32 Oxygen contents before (O_i) and after (O_f) vacuum decarburization. *From Ref. 2.*

After approximately 20 min treatment time, the final oxygen content of the steel is always high when the initial content is high (low initial carbon content) in both the tank degasser and the RH, Fig. 11.32.[2]

It can be seen from Fig. 11.32 that the decrease in oxygen content of the steel as a result of the vacuum decarburization treatment is less than that expected from the stoichiometry of reaction 11.5.1. This is because there is oxygen transfer from the ladle slag to the steel during vacuum decarburization. Another source of oxygen is the iron oxide-rich skull which builds up on the inside of the vacuum vessel as a result of previous operations. Thus, some decarburization via the following reaction takes place also

$$(FeO) + [C] \rightarrow Fe + CO\ (g) \tag{11.5.2}$$

From the stoichiometry of the reactions, the material balance gives the following relation for the quantity of oxygen transferred to the steel from the ladle slag and the oxidized skull inside the vacuum vessel[2]

$$\Delta O\ (slag) = (16/12)\ \Delta([C] - \Delta[O] \tag{11.5.3}$$

where

$$\Delta[C] = [\%C]_i - [\%C]_f$$

$$\Delta[O] = [ppm\ O]_i - [ppm\ O]_f$$

The values of ΔO (slag) derived from the plant data using equation 11.5.3 are shown in Fig. 11.33.[2] It is seen that during decarburization the amount of oxygen transferred from slag to steel is higher the higher the initial carbon content. For initial carbon contents of 200 ppm or less there is no more oxygen pickup from the slag during vacuum decarburization and the carbon content decreases according to the stoichiometry of reaction 11.5.1.

11.5.2.1 Rate of Decarburization

The rate of decarburization is expressed by the following relationship

$$\ln\left\{\frac{[\%C]_f}{[\%C]_i}\right\} = -k_C t \tag{11.5.4}$$

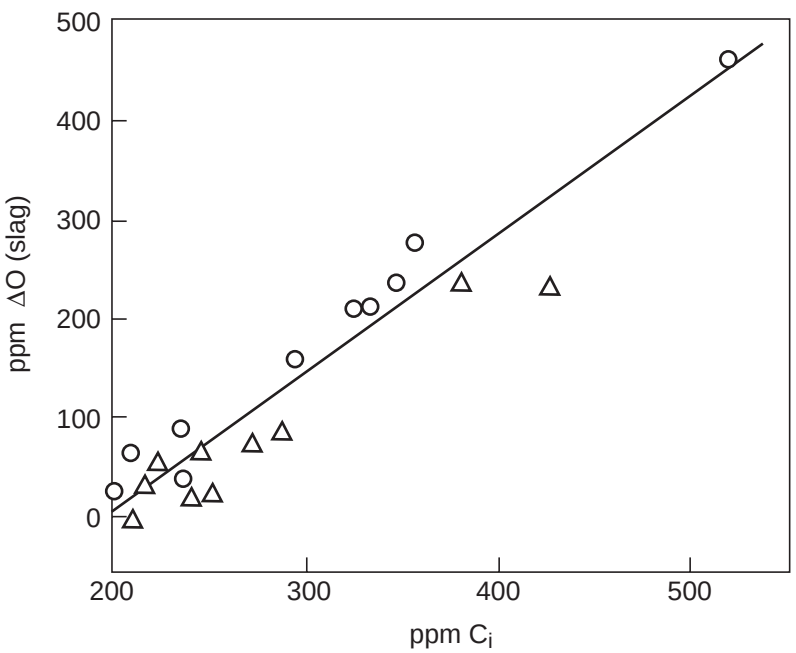

Fig. 11.33 Transfer of oxygen from ladle slag to steel during decarburization in tank degassers (triangles) and in RH degassers (circles). *From Ref. 2.*

where $[\%C]_i$ and $[\%C]_f$ are the carbon contents before and after decarburization, respectively and k_C is the rate constant for decarburization. For RH degassers the rate constant is given by the following relationship

$$k_C = \frac{Q}{V_b \rho} \frac{q}{\frac{Q}{\rho} + q}, \ \text{min}^{-1} \tag{11.5.5}$$

where

Q	=	circulation rate of liquid steel, kg/min
V_b	=	volume of the steel bath in the ladle, m^3
ρ	=	density of liquid steel, kg/m^3
q	=	volumetric mass transfer coefficient of decarburization, m^3/min

According to Kuwabara et al.[70] the circulation rate of the liquid steel in the RH vessel is given by

$$Q\ (\text{tonne / min}) = 11.4\left(\dot{V}\right)^{1/3}(D)^{4/3}\left[\ln\left(\frac{P_1}{P_0}\right)\right]^{1/3} \tag{11.5.6}$$

where

$\dot{V}$	=	flowrate of argon injected into the up-leg snorkel, Nl/min
D	=	inside diameter of the up-leg snorkel, m
P_1, P_0	=	pressure at the argon injection point and at the bath surface, respectively, Pa.

The volumetric mass transfer coefficient of decarburization, q, is proportional to the cross sectional area, A_v, of the vessel which is equivalent to the surface area of the bath. From plant observations on 240 to 300 tonne RH vessels Kato et al.[71] found the following approximate empirical relationship for q:

$$q = 0.26\, Q^{0.64}\, A_v\, [\%C] \tag{11.5.7}$$

valid for $0.0025 \leq [\%C] \leq 0.01$.

It should be noted that the actual rate is very complex. The reaction occurs at various sites including the argon bubble surface, refractory surfaces, metal free surfaces, and homogeneously in the melt. Therefore, equation 11.5.7 should only be used for similar conditions for which it was developed.

According to the above equations, the rate of decarburization will increase with snorkel diameter and vessel diameter, which was confirmed by actual plant data.[71]

In Fig. 11.34 the decarburization rate constant, k_C, is shown as a function of the specific flowrate (Nm^3/min tonne) of the stirring gas for recirculating systems such as RH and DH and for non-recirculating systems such as VAD.[69] Because of the lower specific flowrates for the stirring gas used in non-recirculating systems, the time required to remove 50% of the carbon is approximately 7 min, whereas in the RH this time can be as short as 3 to 4 min, Fig. 11.34.

Several methods to enhance the decarburization rate in the RH have been reported.[25] Kuwabara et al.[70] were able to increase the decarburization rate by injecting argon through nozzles installed in the hearth of the RH vessel. By injecting argon at a rate of 400–500 Nl/min the carbon content in a 100 tonne heat of steel was decreased from 200 to approximately 10 ppm in 20 min, corresponding to $k_C \approx 0.15\ \text{min}^{-1}$ as found from equation 11.5.4. This is approximately 50% higher than k_C for a conventional RH, Fig. 11.34.

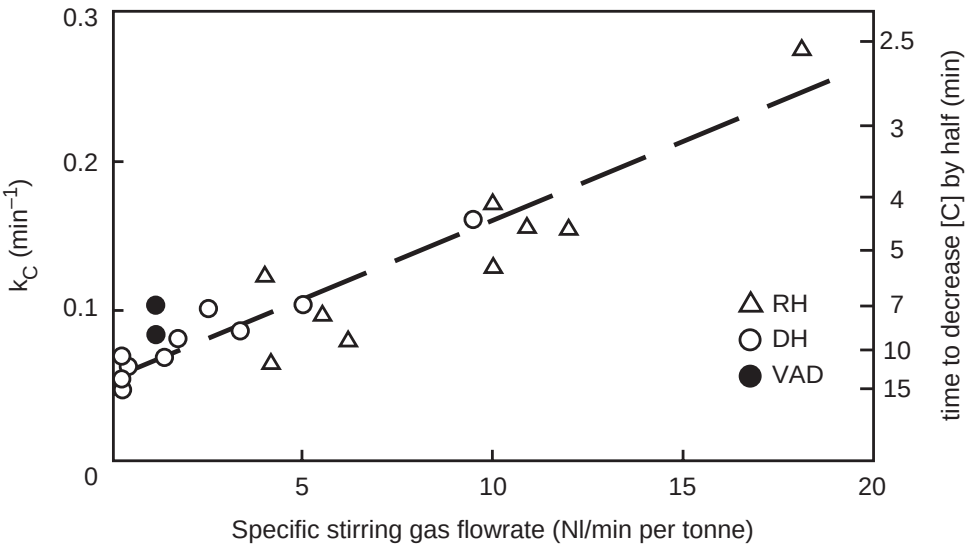

Fig. 11.34 Decarburization rate constant as affected by the specific flowrate of the stirring gas for recirculating systems (RH, DH) and non-recirculating systems (VOD). *From Ref. 69.*

Yamaguchi et al.[72] co-injected hydrogen and argon into the up-leg of the RH to attain 6 ppm hydrogen in the steel. The vessel was then evacuated while the injection of hydrogen continued. The evolution of hydrogen gas bubbles within the bath resulted in a final carbon content of 5–10 ppm.

Okada et al.[73] reported that top blowing of powders onto the surface of the bath in the RH—the so-called RH-PB (powder blowing) process—is effective for attaining ultra low carbon, nitrogen and sulfur contents. For example, by blowing 20–60 kg/min of iron ore powder (–100 mesh) through a top lance positioned 2–3m above the bath surface the final carbon content attained was less than 5 ppm.

Whenever the initial carbon content of the steel is relatively high, the decarburization rate may be limited by the supply of oxygen. To remedy this, the RH-OB (oxygen blowing) and RH-KTB (Kawasaki Top Blowing) processes were developed. In the RH-OB process the oxygen is supplied via tuyeres installed in the sidewalls in the lower part of the RH vessel.[74] In the RH-KTB process the oxygen is supplied via a lance situated in the RH vacuum vessel.[25] In these configurations of the RH process skull formation inside the vessel has been minimized by post combustion of the CO by the injected oxygen.

Yamaguchi et al.[75] developed a reaction model for decarburization in the RH and RH-KTB processes which is based on a mixed control mechanism involving the mass transfer of carbon and oxygen in the liquid steel present in the vacuum vessel as well as on the transport of carbon and oxygen by the recirculating steel. The model satisfactorily takes into account the effect of the concentration of oxygen on the decarburization rate in the conventional RH as well as in the RH-KTB process.

11.5.3 Hydrogen Removal

The rate of hydrogen removal during degassing is controlled by mass transfer in the liquid steel for which the rate equation is given by

$$\ln\left\{\frac{[H]_f - [H]_e}{[H]_i - [H]_e}\right\} = -k_H t \qquad (11.5.8)$$

where

$[H]_f$ = the hydrogen content after degassing

$[H]_i$ = the initial hydrogen content

$[H]_e$ = the equilibrium hydrogen content as determined by the pressure in the system

k_H = the overall rate constant for hydrogen removal.

In the majority of modern degassers the attainable pressure is below 0.01 atm (~10 torr) and, consequently, $[H]_e$ can be neglected with respect to $[H]_i$ and $[H]_f$. This gives the following simplified rate equation

$$\ln\left\{\frac{[H]_f}{[H]_i}\right\} = -k_H t \tag{11.5.9}$$

Bannenberg et al.[76] developed a mathematical model for hydrogen removal in a 185 tonne tank degasser. The agreement between the hydrogen content measured after degassing and that calculated from the model is excellent, as shown in Fig. 11.35.The model is based on fundamental principles. The most critical parameter is the bubble size, which is extremely difficult to predict. Therefore, the model should only be used to make comparisons for similar operating conditions.

Using the model, Bannenberg et al.[76] calculated hydrogen removal rates for initial hydrogen contents varying between 3 and 7 ppm and argon flowrates of 0.9 and 1.8 Nm^3/min. The results are summarized in Fig. 11.36 from which it can be seen that it takes 2 to 3 min longer to achieve a given degree of hydrogen removal for steels initially containing 3 ppm hydrogen than for steels initially containing 7 ppm hydrogen. Moreover, it is noted that doubling the flowrate of the argon stirring

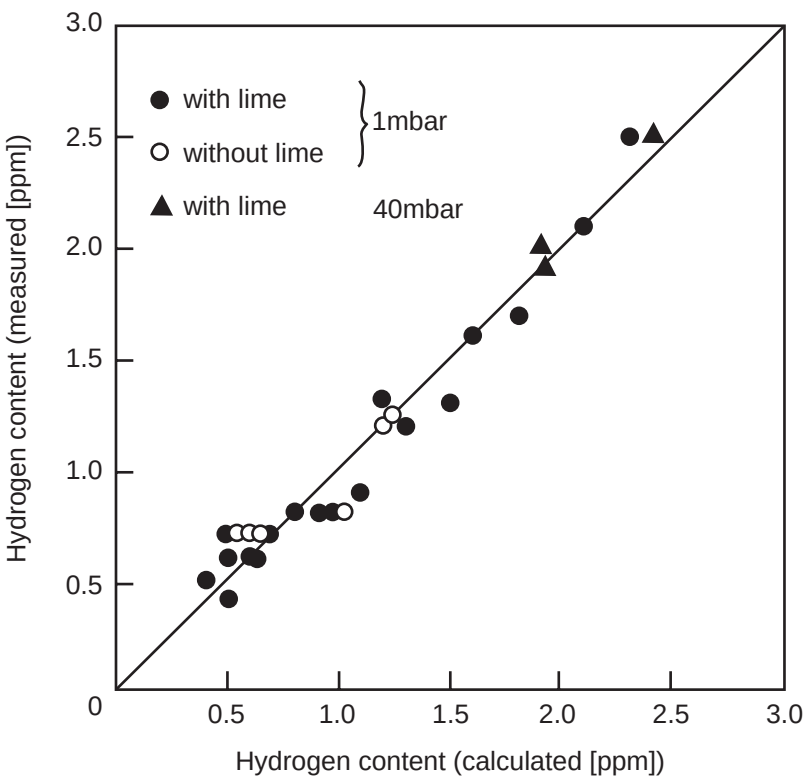

Fig. 11.35 Hydrogen content of the steel measured after vacuum treatment compared with that calculated from a model developed for tank degassing. *From Ref. 76.*

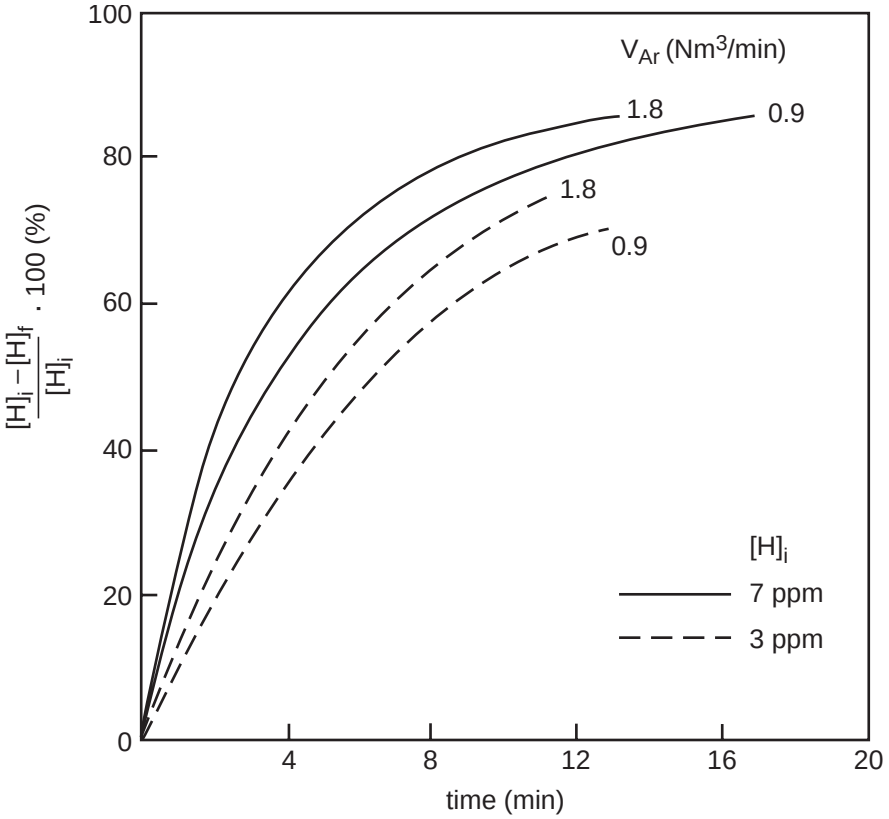

Fig. 11.36 Hydrogen removal for two values of the initial hydrogen content and two argon flowrates in a 185 tonne tank degasser, based on a model developed by Bannenberg et al.[76]

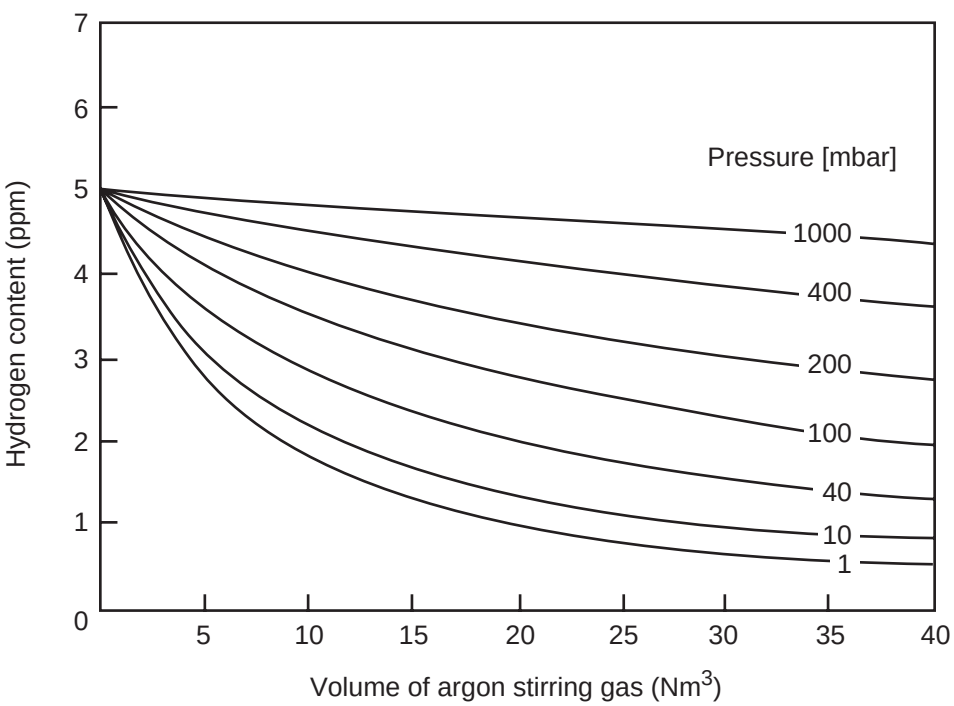

Fig. 11.37 Rate of hydrogen removal in a 185 tonne tank degasser as affected by the tank pressure. *From Ref. 76.*

gas results in a marginally shorter treatment time, e.g. approximately 2 min shorter to achieve 70% hydrogen removal.

Hydrogen removal rates for tank pressures ranging from 1 to 1000 mbar (~10^{-1} atm) are shown as a function of the total volume of argon stirring gas flowing at 1.8 Nm^3/min in Fig. 11.37. It is seen that the final hydrogen content of the steel is essentially unaffected by the tank pressure for pressures up to 10 mbar (~10^{-2} atm).

From the data depicted in Fig. 11.36 it is found that the overall rate constant for hydrogen removal, k_H, increases from approximately 0.09 to 0.16 min^{-1}, when the argon flowrate increases from 0.9 to 1.8 Nm^3/min. The higher k_H value is comparable to the value of 0.13 min^{-1} observed for a RH vessel[2] with a 600 mm diameter snorkel and a steel circulation rate of approximately 140 tonne/min. These values indicate that the efficiencies of recirculating and non-recirculating systems for the removal of hydrogen are similar.

11.5.3.1 Hydris Probe

In shops where hydrogen-sensitive steel grades such as, for example, large bars, are produced, it is important to know the hydrogen content of the steel bath before it is delivered to the caster or the teeming platform. Under such circumstances an in-site determination of the hydrogen content of the bath in the ladle may be desirable.

Around ten years ago, Plessers et al.[79] described an immersion system, the Hydris probe, for the rapid in-situ determination of hydrogen in a bath of liquid steel. The principle of the measurement is based on equilibrating a known volume of argon, being passed through the liquid steel, with the hydrogen dissolved in the steel. Thus, the argon–hydrogen gas mixture leaving the steel after equilibration has a partial pressure of hydrogen that, via Sieverts' law (equation 2.4.8), can be related to the hydrogen content of the steel. The Hydris probe was tested extensively by Frigm et al.[80] who found that it gave reliable readings of the hydrogen content of the liquid steel with an uncertainty of approximately ±5%.

The Hydris probe has been in regular use at the Faircrest steel plant of The Timken Company for a number of years and has been found to be rugged and reliable. The cost associated with the use of the probe has to be weighed against cost savings made possible by its use such as, for example, a significant decrease in degassing time to attain the required hydrogen content in the steel.

11.5.4 Nitrogen Removal

Some nitrogen removal from liquid steel during vacuum degassing is possible, provided the steel is fully killed and has a low sulfur content. Bannenberg et al.[76] developed a rate equation for nitrogen removal in a 185 tonne tank degasser which was based on a mixed-control model, i.e. liquid-phase mass transfer of nitrogen to the argon bubbles coupled with chemical reaction control at the liquid-gas bubble interface. As shown in Fig. 11.38, the nitrogen contents after degassing calculated from the model and indicated by the solid lines, are in good agreement with the measured nitrogen contents indicated by the different symbols. Equally good agreement between calculated and measured values was found for steels containing between 20 and 200 ppm sulfur.[77]

The rate of nitrogen removal for various initial nitrogen contents as calculated from Bannenberg's model is shown in Fig. 11.39 for a killed steel containing 2 ppm dissolved oxygen and 10 ppm sulfur and a tank pressure of 1 mbar (~10^{-3} atm). It can be seen that under these conditions approximately 50% of the nitrogen can be removed in roughly 15 min, provided the initial nitrogen content is 50 ppm or higher.

The effect of the steel sulfur content on the rate of nitrogen removal as calculated from Bannenberg's model is shown in Fig. 11.40. As with the hydrogen case, the model must be used carefully due to the uncertainty in bubble size.

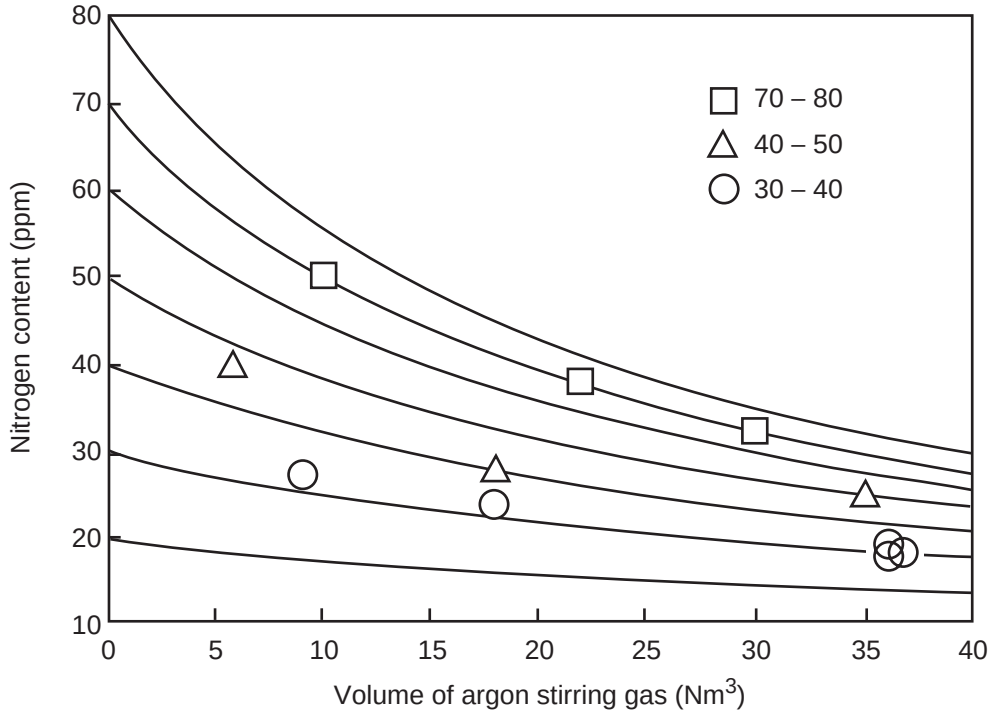

Fig. 11.38 Calculated rates of nitrogen removal in a 185 tonne tank degasser compared with measured data (symbols) for steels containing less than 20 ppm sulfur. *From Ref. 77.*

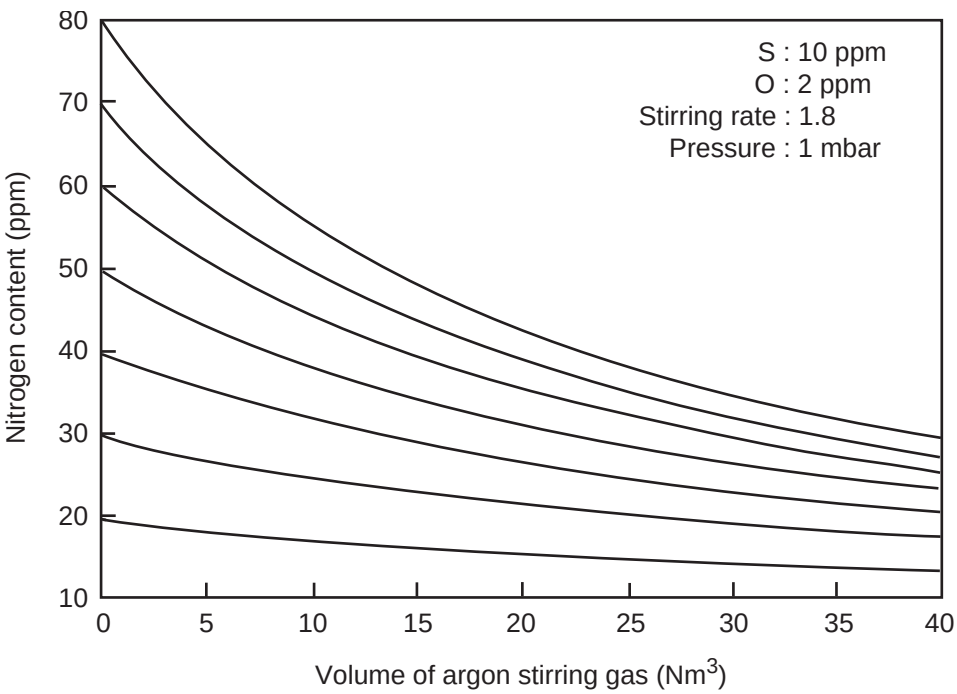

Fig. 11.39 Rates of nitrogen removal in a 185 tonne tank degasser calculated from a model. *From Ref. 76.*

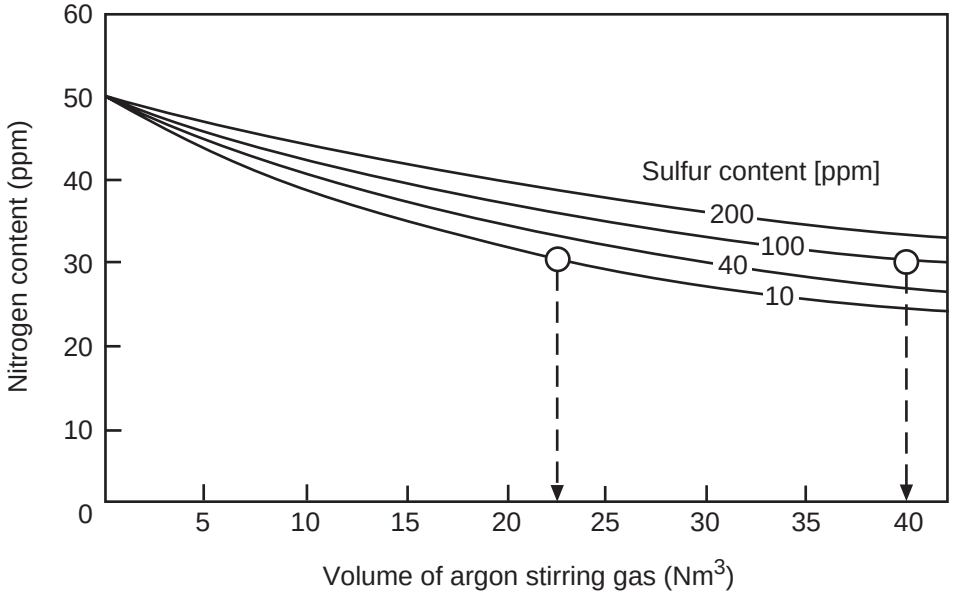

Fig. 11.40 Rates of nitrogen removal in a 185 tonne tank degasser as affected by the steel sulfur content. *From Ref. 78.*

A simplified form of the rate equation for nitrogen removal, equation 2.2.58 is:

$$\frac{1}{\text{ppm N}} - \frac{1}{\text{ppm N}_o} = k_N\,(1-\Theta)\,t \qquad (11.5.10)$$

where k_N is the apparent rate constant for denitrogenization for the limiting case in which both the oxygen and sulfur contents tend to zero. From the nitrogen removal rates shown in Fig. 11.40, together with equation 2.2.56 for $(1 - \Theta)$, the apparent rate constant is estimated to be $k_N \approx 0.0013$ (ppm N min) $^{-1}$ for 185 tonne heats in a tank degasser at 1 mbar (~10^{-3} atm) pressure.

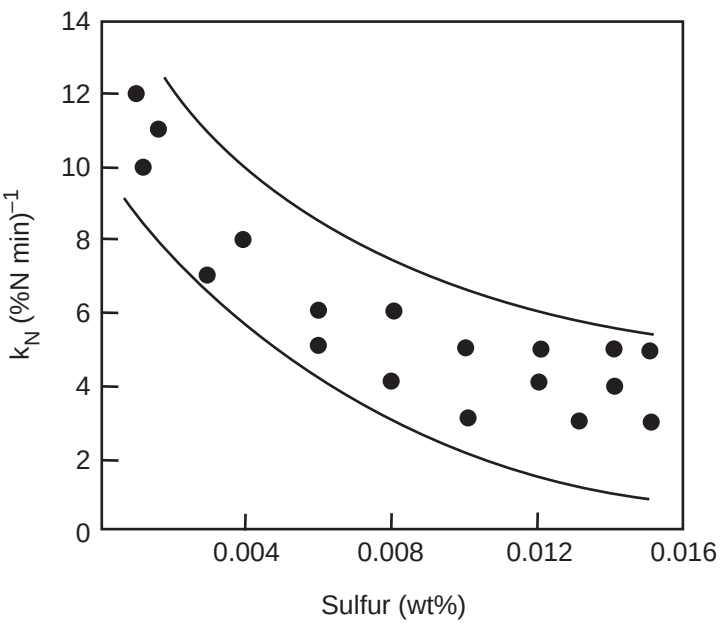

Fig. 11.41 Overall rate constant for nitrogen removal in a RH degasser as affected by the steel sulfur content. *From Ref. 81.*

The overall rate constant for denitrogenization in a RH degasser[81] is shown as a function of the sulfur content of the steel in Fig. 11.41. It is noted that the value of k_N for sulfur contents approaching zero is very similar to the aforementioned value for a tank degasser. Thus, from these values it is concluded that recirculating and non-recirculating degassers are equally effective in removing nitrogen as well as hydrogen (Section 11.5.3).

Recently, an on-line method for the determination of the nitrogen content of liquid steel has been developed.[89] The system, called Nitris, is based on the

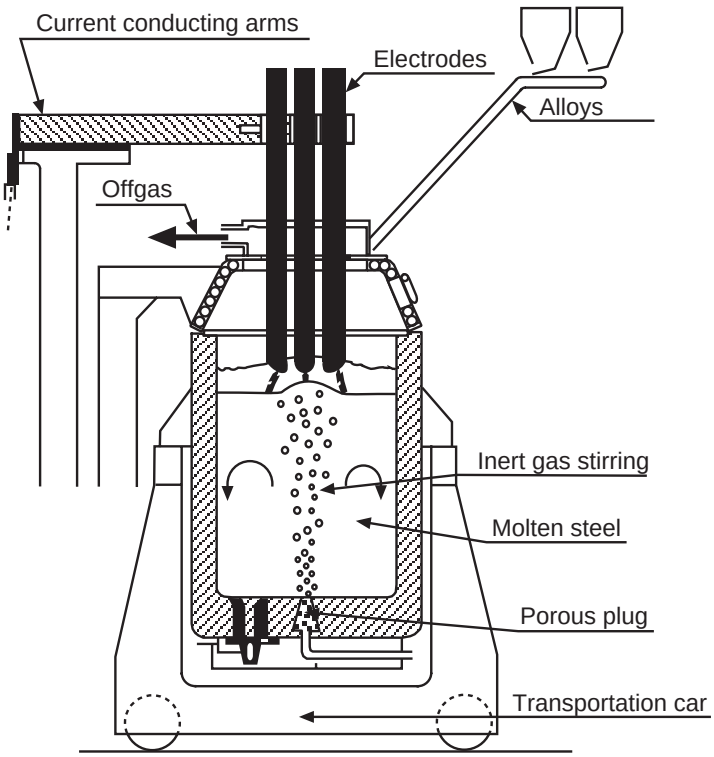

Fig. 11.42 Schematic illustration of a Daido ladle furnace as modified by Fuchs System-technik. *From Ref. 84.*

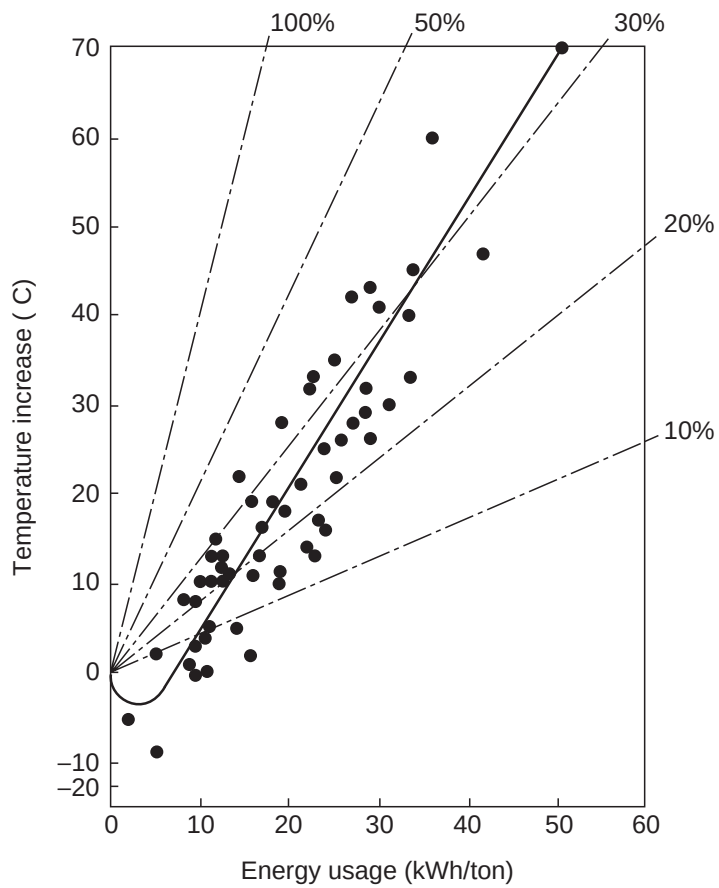

Fig. 11.43 Temperature increase in a 45 tonne ladle furnace as affected by the specific energy input. *From Ref. 84.*

same measuring principle as the Hydris probe, discussed in Section 11.5.3. Jungreithmeier et al.[89] presented details on plant data obtained with the Nitris system as well as a comparison with nitrogen contents obtained by means of the traditional combustion method.

11.6 Description of Selected Processes

In this section a more detailed description of the most popular processes used in secondary steelmaking operations will be presented. Other, less popular, processes are described in several review papers.[1, 68, 82] This section is concluded with some general remarks concerning process selection.

11.6.1 Ladle Furnace

Ladle furnaces are among the most widely used pieces of equipment in secondary steelmaking operations and range from relatively simple retrofitted installations[83] to elaborately equipped facilities. An example of the latter category is the ladle furnace as originally developed by Daido Steel Co., shown schematically in Fig. 11.42.[84]

The ladle furnace illustrated in Fig. 11.42 is lined with a basic lining and covered with a water-cooled roof. The bath in the ladle is heated with the aid of three electrodes which are supported by current conducting arms. The process is usually operated with a slag cover on the bath, thus avoiding excessive wear of the ladle lining due to arc radiation. Another advantage of this mode of operation is that a relatively long arc can be employed, resulting in increased energy efficiency and lower specific electrode consumption. During reheating the bath is continually stirred by means of inert gas supplied via a porous plug in the ladle bottom.

The efficiency of reheating a 45 tonne heat of steel in a ladle furnace is shown in Fig. 11.43.[84] The reheating efficiency is between 20 and 30%, depending on the specific energy input. For larger heat sizes the efficiency can be expected to be higher.

An example of the use of a ladle furnace in conjunction with a degasser is given by Bieniosek.[85] The installation and operation of a low budget ladle metallurgy facility at USS/Kobe Steel is discussed by Mobberly and Diederich.[86]

11.6.2 Tank Degasser

Steel can be treated in a tank degasser without arc reheating. This is shown schematically in Fig. 11.44 for two different stirring systems. An inductively stirred bath is shown in Fig. 11.44(a) while in Fig. 11.44(b) the bath is stirred by bubbling argon through a porous plug located in the ladle bottom.

11.6.3 Vacuum Arc Degasser

A vacuum arc degasser (VAD) is a tank degasser with electrodes added for the purpose of reheating the steel. A schematic illustration of a VAD unit is shown in Fig. 11.45.

Whittaker[87] described a VAD process used at Atlas Specialty Steels in which two ladle covers are used sequentially, shown schematically in Fig. 11.46. During reheating the ladle is placed underneath a water cooled steel roof fitted with three electrodes. The cover is not designed to operate under vacuum. For degassing the ladle is placed underneath a roof fitted with a sight port, vacuum offtake and a water-cooled O-ring seal. This seal makes the system gastight such that the final pressure inside the ladle can be less than 1 torr (~0.0013 atm). For processing stainless steels the oxygen lance is used and the unit is operated as a VOD.

Another VAD unit that operates with a gastight ladle cover is the Stein-Heurtey–S.A.F.E. System.[88] Two such units are in operation at The Timken Company's steel plants where heat sizes between approximately 120 and 160 tonnes are processed.

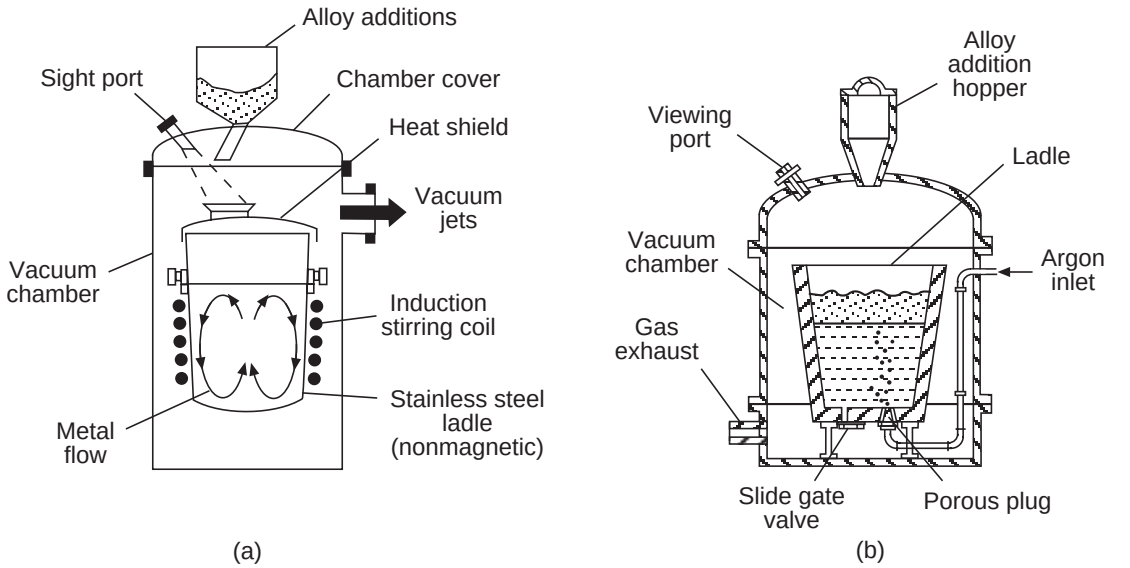

Fig. 11.44 Two types of tank degasser: (a) induction coil stirring, (b) porous plug for argon bubbling. *From Ref. 2.*

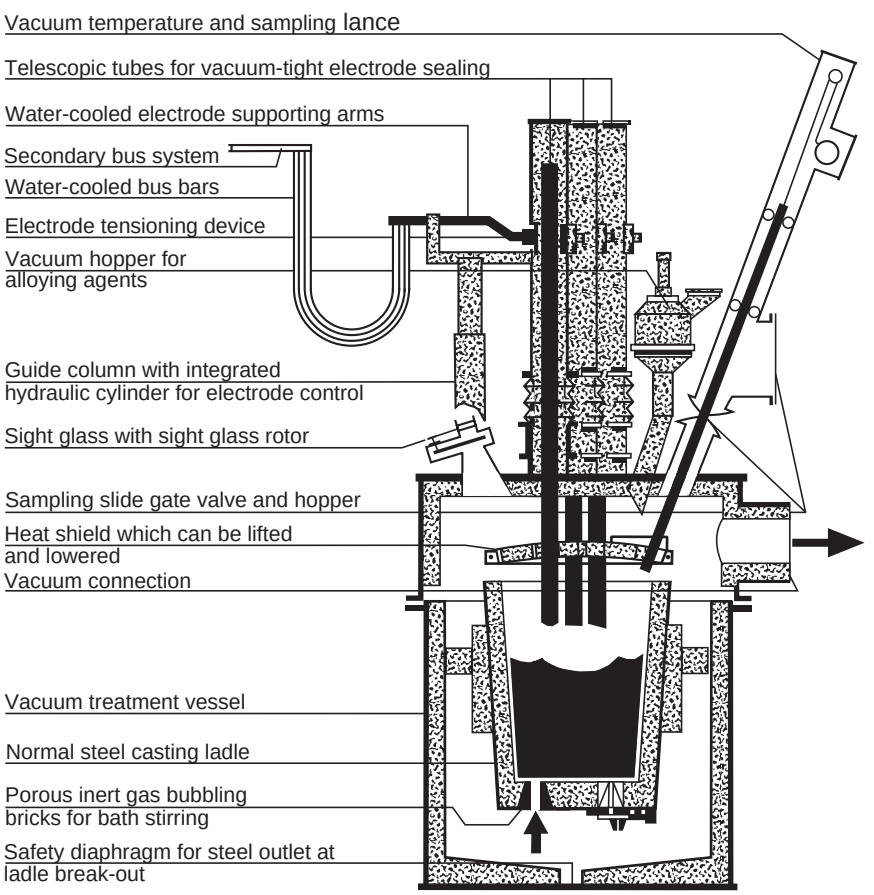

Fig. 11.45 Schematic illustration of a VAD unit. *From Ref. 68.*

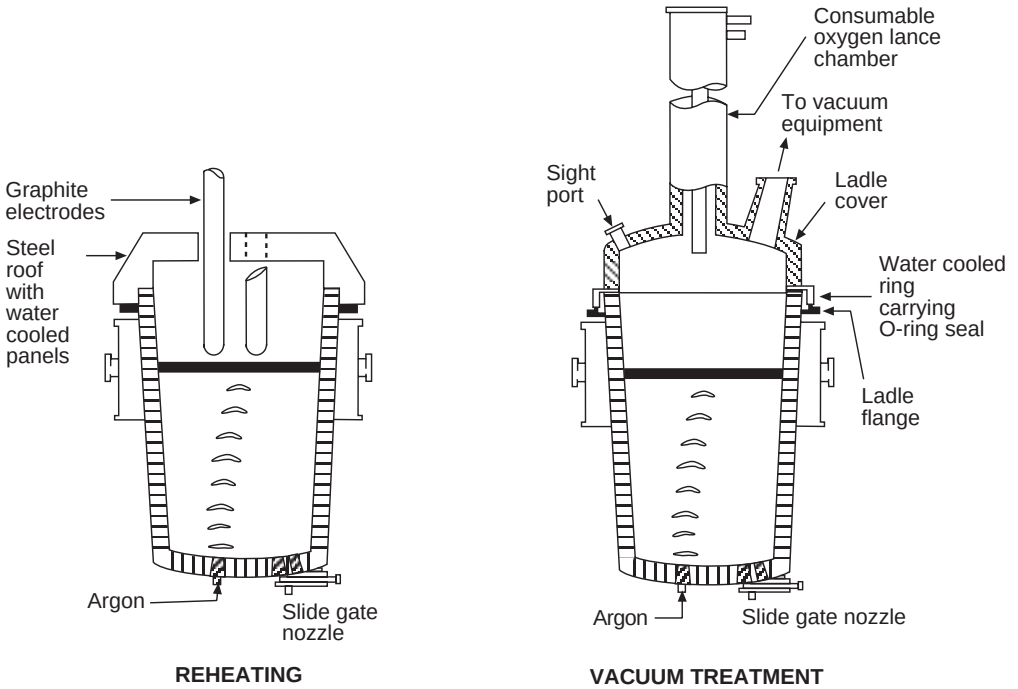

Fig. 11.46 Schematic illustration of the use of separate ladle covers for reheating and degassing of 68 tonne heats at Atlas Specialty Steels. *From Ref. 87.*

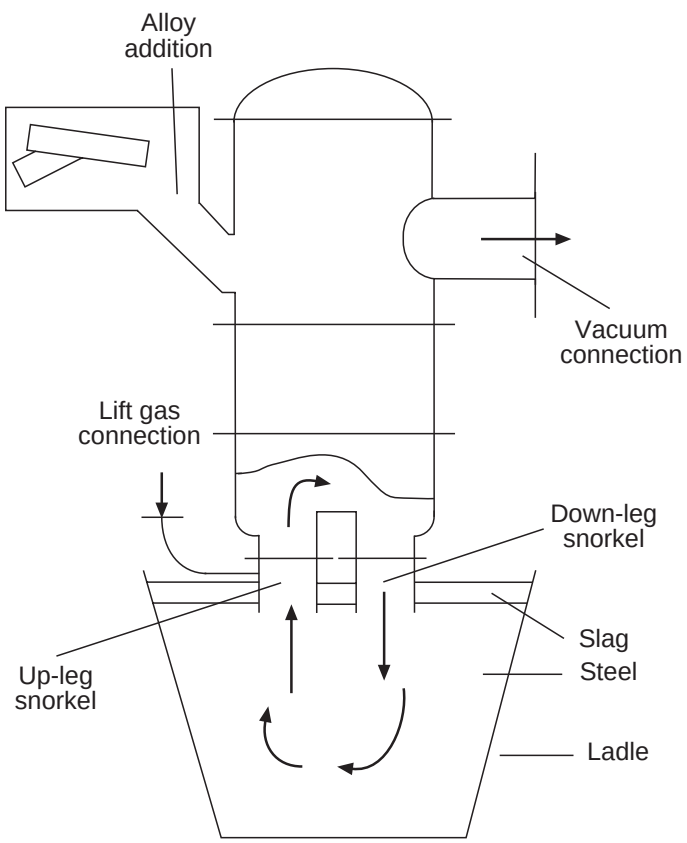

Fig. 11.47 Schematic illustration of the principle of the RH process. *From Ref. 92.*

Process control systems for the ladle metallurgy facilities at Dofasco and at LTV's Indiana Harbor plant were described by Brown et al.[90] and by Rada and Clarkson[91], respectively.

11.6.4 RH Degasser

A schematic illustration of the principle of the RH process is depicted in Fig. 11.47[92] while a sketch of a RH unit with ancillary equipment is shown in Fig. 11.48.[93] The 145 tonne RH unit shown in Fig. 11.48 was designed for a monthly steel production of 40,000 tonne, approximately 30% of which represents ULC-IF steel grades.

To increase the availability of the RH installation, many steel shops operate the facility with two vessels, one of which will be in the operating position while the other is being repaired or relined. The operation of such a two-vessel facility at Inland Steel Co. was discussed by Schlichting and Dominik.[94]

Over the years the RH process was developed further with the aim to enhance the capabilities of the process. One of the important developments was the addition of oxygen to the RH vessel, either by injection through a tuyere mounted in the sidewall of the vessel (RH-OB) or via a top lance inside the vessel (RH-KTB).

Because of the violent splashing occurring inside the RH vessel, skull formation on its inside walls results. In the RH-KTB process the skull formation is minimized as a result of the heat generated by the post combustion of CO to CO_2, as schematically illustrated in Fig. 11.49.

To enhance the capabilities of the RH process even further, the RH-PB (powder blowing) process was developed. The addition of powder and/or fluxes makes it possible to desulfurize or dephosphorize the steel during the RH operation. Kuwabara et al[96] have reported on the injection of fluxes into the lower part of the ladle during the operation of a RH unit.

Fujii et al.[95] studied the effect of fluid flow on the decarburization rate in a RH degasser and related this to design parameters such as the snorkel and vessel diameters as well as the circulation flowrate. A control model for the RH degasser was discussed by Sewald[92] with emphasis on the

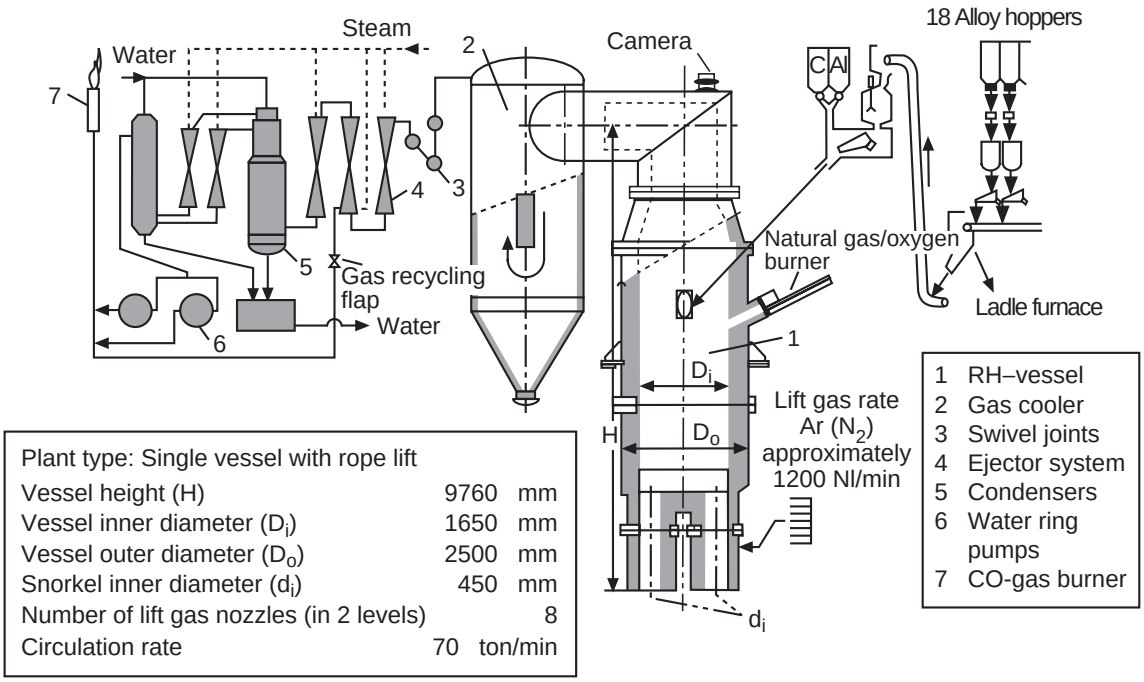

Plant type: Single vessel with rope lift		
Vessel height (H)	9760	mm
Vessel inner diameter (D_i)	1650	mm
Vessel outer diameter (D_o)	2500	mm
Snorkel inner diameter (d_i)	450	mm
Number of lift gas nozzles (in 2 levels)		8
Circulation rate	70	ton/min

Fig. 11.48 Schematic illustration of a 145 tonne RH unit with ancillary equipment as installed in the LD steel plant of Voest-Alpine Stahl, Linz, Austria. *From Ref. 93.*

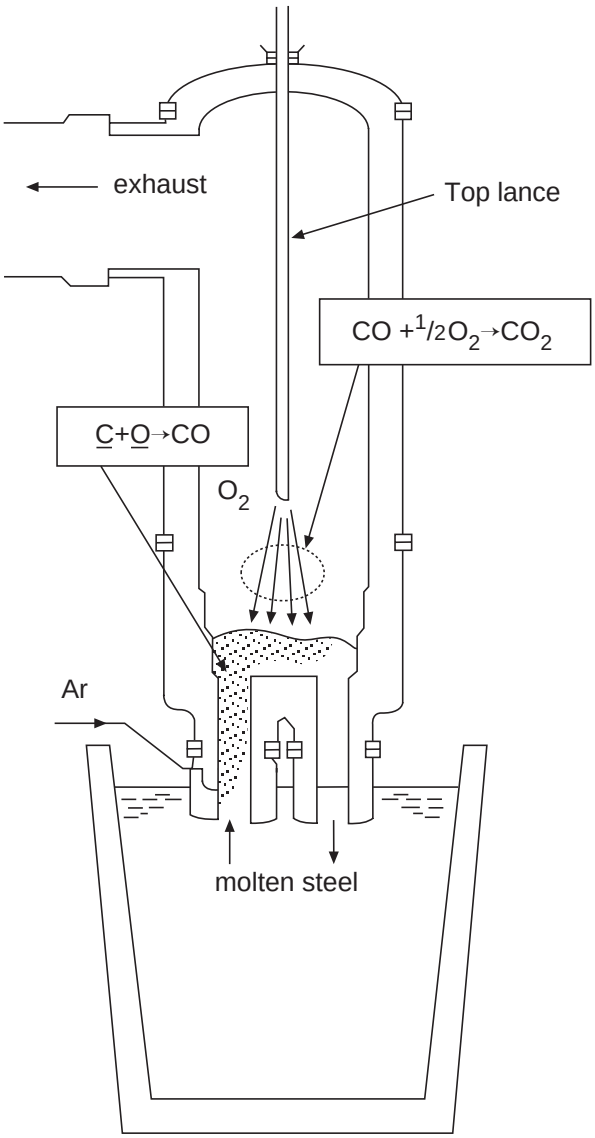

Fig. 11.49 Schematic illustration of the the RH-KTB process. *From Ref. 95.*

supervisory computer control system as well as the design and operational characteristics of the process model.

11.6.5 CAS-OB Process

The CAS-OB process (Composition Adjustment by Sealed argon bubbling with Oxygen Blowing) was developed by Nippon Steel Co. and was recently installed at the Steubenville plant of the Wheeling-Pittsburgh Steel Co.[97] A schematic illustration of a CAS-OB unit is shown in Fig. 11.50.

The main feature of the process is the refractory snorkel or bell underneath which alloy additions to the bath are made. The ladle is positioned such that the snorkel is situated right above the porous stirring plug, Fig. 11.50. This ensures that the agitated surface of the steel bath is confined to the area underneath the bell. Additional argon stirring, if necessary, is obtained via a specially shaped submerged lance, Fig. 11.50. Reheating of the steel is accomplished by injecting oxygen through the top lance in conjunction with aluminum additions. For low-carbon steel the rate of reheating in the

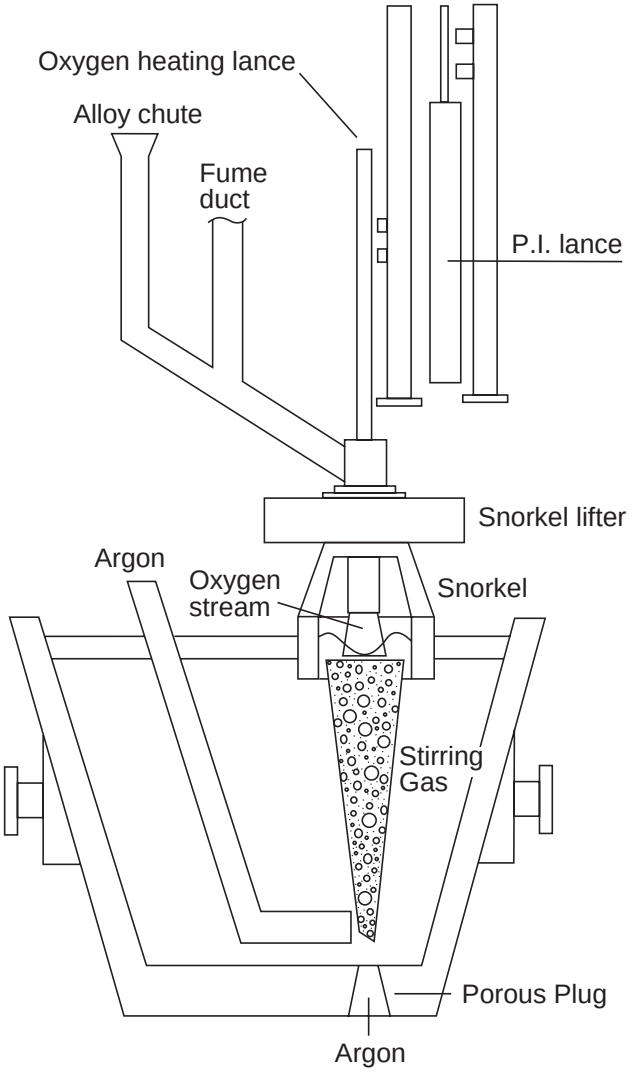

Fig. 11.50 Schematic illustration of a CAS-OB process. *From Ref. 97.*

CAS-OB was found to be approximately 10°C/min[97] (~20°F/min). This is in broad agreement with data reported by Palchetti et al.[98] who observed a similar reheating rate for an oxygen blowing rate of approximately 70 Nm^3/min (~2470 scfm) for 300 tonne heats.

11.6.6 Process Selection and Comparison

Fruehan[68] has addressed the various issues that are involved in the selection of a process, particularly a degassing unit, for a given steel plant. Some of the most important considerations are: future and current product mix; requirements with respect to carbon, hydrogen, nitrogen and sulfur (phosphorus) content of the final product; reheating capability (e.g. does the shop have a ladle furnace); effect on steelmaking facility (BOF or EAF); degassing time compatible with other operations, e.g. with sequential continuous casting; and capital and operating costs.

An important issue is to match the time requirement of the degassing unit to the processing times in the steelmaking furnace (BOF or EAF) and in the continuous caster. For example, to attain a carbon content of 0.005% or less requires 10–15 min in an RH-OB (KTB) compared with 15–20 min in a tank degasser such as a VOD. When such low carbon contents are a frequent requirement, the installation of an RH-OB (KTB) unit is usually warranted.

Another important issue is the demand on the steelmaking furnace. Ultra-low-carbon steels are easier to produce in an RH or tank degasser when the initial carbon content (the tap carbon content) is less than 0.025%. At these low carbon levels the steel contains enough dissolved oxygen to remove the required amount of carbon in a practical time span. However, having to tap the steel at such low carbon contents puts an extra load on the BOF with detrimental ramifications in regard to the vessel lining because of the higher temperature and FeO content of the slag. With an RH-OB (KTB) or VOD it is possible to tap the steel at higher carbon contents because supplemental oxygen is available for enhanced decarburization, as discussed in Section 11.5.2.1.

Table 11.8 may serve as a first approximation to a semi-quantitative comparison of the various vacuum degassing systems[68].

Table 11.8 Comparison of Various Degassing Systems. *From Ref. 68.*

	Type of Degasser				
	RH-OB	**RH**	**VOD**	**Tank**	**Ladle**
Decarburization level (ppm)	20	20	20–30	30–40	30–40
Decarburization rate	Highest	Satisfactory for low carbon	High	Approx. 2–30% slower than RH, RH-OB,VOD	
Decarburization time to 50 ppm min)	10–15	12–15	15–18	15–20	15–20
Hydrogen removal	All systems are reasonably satisfactory				
Inclusion Removal	All systems can improve cleanliness, VOD, tank & ladle require a rinse cycle				
Desulfurization	Only possible with RH injection or RH-PB. (Rarely practiced)			Excellent desulfurization possible but must be separate from decarburization	
Aluminum heating	yes	no	yes	no	no
Relative Capital Cost (RH-OB = 1.0)	1.0	0.7–0.8	0.4–0.6	0.4–0.5	0.3–0.4
Maintenance Cost	Decreasing	⟶	⟶		

References

1. B. R. Nijhawan, *Proc. Emerging Technologies for New Mat. and the Steel Industry* (Cincinnati: October 1991), 215.
2. E. T. Turkdogan, *Fundamentals of Steelmaking*, (London: The Institute of Materials, 1996), Chapter 9.
3. J. Szekely, *Trans. Met. Soc. of AIME* 245 (1969): 314.
4. K. Schwerdtfeger and W. Wepner, *Met. Trans. B*, 8B (1977): 287.
5. P. Massard and K. W . Lange, *Arch. Eisenhuettenw*. 48 (1977): 521.
6. T. Choh, K. Iwata and M. Inouye, *Trans. ISIJ* 23 (1983): 598.
7. P. C. Glaws, G. J. W. Kor, and R. V. Fryan, *Proc. Electric Furnace Conference,* 47 (Warrendale, PA: Iron and Steel Society, 1989), 383.

8. J. Szekely, G. Carlsson, and L. Helle, in *Ladle Metallurgy*, Materials Research and Engineering Series, B. Ilschner and N. J. Grant, eds. (New York: Springer-Verlag, 1988).
9. E. Hoeffken, H. D. Pflipsen, and W. Florin, *Proc. Int. Conf. On Secondary Metallurgy* (Aachen, 1987): 124.
10. R. E. Kracich and K. Goodson, *Iron and Steelmaker* 23, 7 (1996): 41.
11. E. T. Turkdogan, *Ironmaking and Steelmaking* 15 (1988): 311.
12. P. C. Glaws, G. J. W. Kor, The Timken Company, internal reports.
13. R. Engel, R. Marr, and E. Pretorius, *Keeping Current* series, *Iron and Steelmaker*, 23–24 (1996–97).
14. C. E. Tomazin, E. A. Upton, and R. A. Wallis, *Steelmaking Conf. Proc.,* 69 (Warrendale, PA: Iron and Steel Society, 1986), 223.
15. C. Vitlip, *Iron and Steelmaker* 23, 7 (1996): 55.
16. P. E. Anagbo and J. K. Brimacombe, *Iron and Steelmaker* 15, 10 (1988): 38.
17. P. E. Anagbo and J. K. Brimacombe, *Iron and Steelmaker* 15, 11 (1988): 41.
18. W. Pluschkell, *Stahl und Eisen* 101 (1981): 97.
19. D. Mazumdar and R. I. L. Guthrie, *ISIJ Int.*, 35 (1995): 1.
20. D. Mazumdar and R. I. L. Guthrie, *Met Trans. B*, 17B (1986): 725.
21. M. Neifer, S. Roedl, and D. Sucker, *Steel Research*, 64 (1993): 54.
22. M. Sano and K. Mori, *Trans. ISIJ*, 23 (1983): 43.
23. J. Mietz and F. Oeters, *Steel Research*, 60 (1989): 387.
24. S. Joo and R. I. L. Guthrie, *Met. Trans. B*, 23B (1992): 765
25. T. Emi, *Proceedings,* Scaninject VII, part I (1995): 225.
26. S. Asai, M. Kawachi, and I. Muchi, *Proceedings,* Scaninject III, part I (1983): 12:1.
27. Y. Kikuchi et al., *Proceedings,* Scaninject III, part I (1983): 13:1.
28. S. Kim and R. J. Fruehan, *Met. Trans. B*, Vol. 18B (1987): 381.
29. J. Mietz, S. Schneider, and F. Oeters, *Steel Research* 62 (1991): 10.
30. K. Nakanishi and J. Szekely, *Trans. ISIJ* 15 (1975): 522.
31. T. A. Engh and N. Lindskog, Scand. *J. Met.* 4 (1975): 49.
32. K. W. Lange, *Int. Materials Reviews* 33 (1988): 53.
33. R. Ruddelston et al., *Ironmaking and Steelmaking* 18 (1991): 41.
34. J. A. Eckel, The Timken Company, private communication.
35. J. K. Cotchen, *Int. Symp. On Ladle Steelmaking and Furnaces,* (Montreal: The Met. Soc. of CIM, 1988): 111.
36. J. A. Barbus et al., *Steelmaking Conf. Proc*., 72 (Warrendale, PA: Iron and Steel Society, 1989), 23.
37. Y. Miyashita and Y. Kikuchi, *Proc. Int. Conf. On Secondary Metallurgy* (Aachen, 1987), 195.
38. C. J. Bingel, LTV Steel Co., private communication, 1997.
39. N. R. Griffing et al., *Proc. Electric Furnace Conf.*, Vol. 46 (Warrendale, PA: Iron and Steel Society, 1988), 301.
40. E. T. Turkdogan, *JISI* 210 (1972): 21.
41. R. K. Iyengar and G. C. Duderstadt, *Trans. Met. Soc. AIME* 245 (1969): 807.
42. A. Thomas, F. Villette and F. J. Piton, *Iron and Steel Engineer* 63, 2 (1986): 45.
43. S. Dimitrov, A. Weyl and D. Janke, *Steel Research* 66 (1995): 3.
44. E. Schuermann et al., *Arch. Eisenhuettenw* 50 (1979): 139.
45. P. Riboud and R. Vasse, *Rev. de Métallurgie–C.I.T.,* 82 (1985): 801.
46. Y. Hara et al., *Proceedings,* Scaninject IV, part I (1986), 18:1.
47. I. Sawada, T. Kitamura, and T. Ohashi, *Proceedings,* Scaninject IV, part I (1986), 12:1.
48. C. A. Abel, R. J. Fruehan, and A. Vassilicos, *Trans ISS, Iron & Steelmaker* 22, 8, (1995): 49.
49. P. V. Riboud and C. Gatelier, *Ironmaking and Steelmaking*, 12 (1985): 79.
50. G. Becker et al., *Rev. de Métallurgie–C.I.T.*, 81 (1984): 857.
51. N. Bannenberg and H. Lachmund, *Rev. de Métallurgie–C.I.T.*, 91 (1994):1043.
52. G. Jung et al., *Process Technology Proc.,* 14 (Warrendale, PA: Iron and Steel Society, 1995), 109.
53. S. A. Argyropoulos and R. I. L. Guthrie, *Steelmaking Conf. Proc.,* 65 (Warrendale, PA: Iron and Steel Society, 1982), 156.

54. Y. E. Lee, H. Berg, and B. Jensen, *Ironmaking and Steelmaking* 22 (1995): 486.
55. D. Mazumdar and R. I. L. Guthrie, *Met. Trans. B* 24B (1993): 649.
56. A. L. Gueussier et al., *Iron and Steel Engineer* 60, 10 (1983): 35.
57. A. Herbert et al., *Ironmaking and Steelmaking* 14 (1987): 10.
58. J. Schade, S. A. Argyropoulos, and A. McLean, *ISS Trans.* 12 (1991): 19.
59. O. P. Watts, *J. Am. Chem. Soc.* 28 (1906): 1152.
60. T. Ototani, in *Calcium Clean Steel*, Materials Research and Engineering Series (B. Ilschner and N. J. Grant, eds.),(New York: Springer Verlag, 1986).
61. R. H. Rein and J. Chipman, *Trans. Met. Soc. AIME* 233 (1965): 415.
62. B. Ozturk and E. T. Turkdogan, *Met. Sci.* 18 (1984): 299.
63. G. J. W. Kor, Elliott Symp. Proc. (P. J. Koros and G. R. St. Pierre, eds.), (Warrendale, PA: Iron and Steel Society, 1990), 479.
64. K. Larsen and R. J. Fruehan, *ISS Trans.* 12 (1991): 125.
65. E. T. Turkdogan, *Process Technology Proc.* 6 (Warrendale, PA: Iron and Steel Society, 1986), 767.
66. R. Aitken, *JISI*, 1886, I, 109.
67. J. H. Flux, *Vacuum Degassing of Steel*, Special Report No. 92, (London: Iron and Steel Institute, 1965).
68. R. J. Fruehan, *Vacuum Degassing of Steel*, (Warrendale, PA: Iron and Steel Society, 1990).
69. N. Bannenberg, P. Chapellier, and M. Nadif, *Stahl und Eisen*, Vol. 113, No. 9 (1993), 75.
70. T. Kuwabara, et al., *Trans. ISIJ* 28 (1988): 305.
71. Y. Kato et al., *Tetsu-to-Hagané* 79 (1993): 1248.
72. K. Yamaguchi, T. Sakuraya, and K. Hamagami, *Kawasaki Steel Giho* 25 (1993), 283.
73. Y. Okada et al, *Proc. 8th Japan-Germany Seminar* (Sendai, October 1993): Tokyo, *ISIJ,* 81
74. B. A. Otterman, R. J. Hale, and R. Merk, *Steelmaking Conf. Proc.* 73 (Warrendale, PA: Iron and Steel Society, 1990), 69.
75. K. Yamaguchi et al., *ISIJ Int.* 32 (1992): 126.
76. N. Bannenberg, B. Bergmann, and H. Gaye, *Steel Research* 63 (1992): 431.
77. B. Bergmann, N. Bannenberg, and H. Gaye, *Rev. de Métallurgie–C.I.T.,* 86 (1989): 907.
78. N. Bannenberg et al., *Proc. 6th Int. Iron and Steel Congr.* 3 (Nagoya, 1990), *ISIJ,* 603.
79. J. Plessers, R. Maes and E. Vangelooven, *Stahl und Eisen* 108 (1988): 451.
80. G. Frigm et al., *Proc. Electric Furnace Conf.* 48 (Warrendale, PA: Iron and Steel Society, 1990), 83.
81. T. Kishida et al. (Daido Steel Co.), quoted in *Stahl und Eisen* 107 (1987): 894
82. B. Grabner and H. Hoeffgen, *Radex Rundschau* 3 (1985): 581.
83. G. Mischenko and S. V. McMaster, *Iron and Steel Engineer* 71, No. 5 (1994): 49.
84. H. Knapp, *Radex Rundschau* 2 (1987): 356.
85. T. H. Bieniosek, *Iron and Steel Engineer* 72, 7 (1995): 17.
86. M. E. Mobberly and D. J. Diederich, *Iron and Steel Engineer*, Vol. 67, No. 5 (1990): 48.
87. D. A. Whittaker, *Int. Symp. on Ladle Steelmaking and Furnaces,* (Montreal: CIM, 1988), 235.
88. R. J. Fruehan, *Ladle Metallurgy Principles and Practices,* (Warrendale, PA: Iron and Steel Society, 1985).
89. Jungreithmeier, K. Jandl, A. Viertauer and F. Sikula, *Steel Technology Int.*, (1996–97):69.
90. D. L. Brown, J. P. Dixon, and J. N. Stacey, *Iron and Steel Engineer* 67, 5 (1990): 30.
91. R. G. Rada and C. R. Clarkson, *Iron and Steel Engineer* 67, 7 (1990): 38.
92. K. E. Sewald, *Iron and Steel Engineer* 68, 7 (1991): 25.
93. H. Presslinger et al., *Radex Rundschau* 4 (1992): 171.
94. M. Schlichting and M. Dominik, *Iron and Steel Engineer* 66, 3 (1989): 47.
95. T. Fujii, Y. Kato, and T. Sakuraya, *Proceedings,* Scaninject VI (1992), 317.
96. T. Kuwabara et al., *Steelmaking Conf. Proc.* 69 (1986), 293.
97. T. J. Cauchie and T. S. Landon, *Iron and Steel Engineer* 73, 5 (1996): 20.
98. M. Palchetti, P. Buglione, and D. Tegas, *Proc. 6th Int. Iron and Steel Congr*. 3 (Nagoya), *ISIJ,* 159.

